

Entropy-based parametric estimation of spike train statistics

J. C. Vasquez ^{*}, T. Viéville ^{*}, B. Cessac ^{* †}

July 27, 2021

Abstract

We propose a generalisation of the existing maximum entropy models used for spike trains statistics analysis, based on the thermodynamic formalism from ergodic theory, and allowing one to take into account memory effects in dynamics. We propose a spectral method which provides directly the “free-energy” density and the Kullback-Leibler divergence between the empirical statistics and the statistical model. This method does not assume a specific Gibbs potential form. It does not require the assumption of detailed balance and offers a control of finite-size sampling effects, inherent to empirical statistics, by using large deviations results. A numerical validation of the method is proposed and the perspectives regarding spike-train code analysis are also discussed.

Keywords: *Spike train analysis , Higher-order correlation , Statistical Physics , Gibbs Distributions , Maximum Entropy*

PACS: *05.10.-a , 87.19.Io , 87.19.lj*

MCS(2000): *37D35 , 37M25 , 37A30*

1 Introduction

Processing and encoding of information in neuronal dynamics is a very active research field [59], although still much of the role of neural assemblies and their internal interactions remains unknown [55]. The simultaneously recording of the activity of groups of neurons (up to several hundreds) over a dense configuration, supplies a critical database to unravel the role of specific neural assemblies. In complement of descriptive statistics (e.g. by means of cross-correlograms or joint peri-stimulus time histograms), somehow difficult to interpret for a large number of units (review in [8, 37]), is the specific analysis of multi-units spike-patterns, as found e.g. in [1]. This approach develops algorithms to detect common patterns in a data block, as well as performing combinatorial analysis to compute the expected probability of different kind of patterns. The

^{*}INRIA, 2004 Route des Lucioles, 06902 Sophia-Antipolis, France.

email: Juan-Carlos.Vasquez@sophia.inria.fr

[†]Laboratoire J. A. Dieudonné, U.M.R. C.N.R.S. N°6621, Université de Nice Sophia-Antipolis, France.

main difficulty with such type of approaches is that they rely on a largely controversial assumption, Poissonian statistics (see [57, 58, 66]), which moreover, is a minimal statistical model largely depending on the belief that firing rates are essentially the main characteristic of spike trains.

A different approach has been proposed in [66]. They have shown that a model taking into account pairwise synchronizations between neurons in a small assembly (10-40 retinal ganglion cells) describes most (90%) of the correlation structure and of the mutual information of the block activity, and performs much better than a non-homogeneous Poissonian model. Analogous results were presented the same year in [73]. The model used by both teams is based on a probability distribution known as the Gibbs distribution of the Ising model which comes from statistical physics. The parameters of this distribution relating, in neural data analysis, to the firing rate of neurons and to their probability of pairwise synchronisation have to be determined from empirical data. Note that this approach has been previously presented in neuroscience, but in a slightly different and more general fashion, by [45, 39, 46] (it was referred as “log-linear models”). The use of Ising model in neural decoding (especially of visual stimuli) has been largely exploited by several other authors [19, 53, 72, 78]. In particular, it is believed by some of them [19] that the pairwise coupling terms inferred from simultaneous spikes corresponds, in the model, to effective couplings between ganglion cells. In this spirit, computing the parameters of the Ising model would provide an indirect access to ganglion cells connections. In addition, an increasing number of different theoretical and numerical developments of this idea have recently appeared. In particular, in [80], the authors propose a modified learning scheme and thanks to concepts taken from physics, such as heat capacity, explore new insights like the distribution of the underlying density of states; additionally in [61, 60] authors study and compare several approximate, but faster, estimation methods for learning the couplings and apply them on experimental and synthetic data drawing several results for this type of modeling.

However, it might be questionable whether more general form of Gibbs distributions (e.g. involving n -uplets of neurons) could improve the estimation and account for deviations to Ising-model ([72, 80]) and provide a better understanding of the neural code from the point of view of the maximal entropy principle [34]. As a matter of fact, back to 1995, [46] already considered multi-unit synchronizations and proposed several tests to understand the statistical significance of those synchronizations and the real meaning of their corresponding value in the energy expansion. A few years later, [45] generalized this approach to arbitrary spatio-temporal spike patterns and compared this method to other existing estimators of high-order correlations or Bayesian approaches. They also introduced a method comparison based on the Neyman-Pearson hypothesis test paradigm. Though the numerical implementation they have used for their approach presented strong limitations, they have applied this methods successfully to experimental data from multi-units recordings in the pre-frontal cortex, the visual cortex of behaving monkeys, and the somato-sensory cortex of anesthetized rats. Several papers have pointed out the importance of temporal patterns of activity at the network level [41, 83, 69], and recently [78] have shown the insufficiency of Ising model to predict the temporal statistics of the neural activity. As a consequence, a few authors (we know only one reference, [44]) have attempted to define time-dependent Gibbs

distributions on the base of a Markovian approach (1-step time pairwise correlations) and convincingly showed a clear increase in the accuracy of the spike train statistics characterization. Namely, this model produces a lower Jensen-Shannon Divergence, when analyzing raster data generated by a Glauber spin-glass model, but also *in vivo* multineuron data from cat parietal cortex in different sleep states.

To summarize, the main advantages of all these 'Ising-like' approaches are:

- (i) to be based on a widely used principle, the maximal entropy principle [34] to determine statistics from the empirical knowledge of (*ad hoc*) observables;
- (ii) to propose statistical models having a close analogy with Gibbs distributions of magnetic systems, hence disposing of several deep theoretical results and numerical methods (Monte-Carlo methods, Mean-Field approximations, series expansions), resulting in a fast analysis of experimental data from large number of neurons.

However, as we argue in this paper, this approaches presents also, in its current state, fundamental weaknesses:

- (i) The maximal entropy principle leads, in its classical formulation, to a parametric form, corresponding to choosing a finite set of *ad hoc* constraints, which only provides an approximation of the real statistics, while the distance (say measured by the Kullback-Leibler divergence) between the model and the hidden distribution can be quite large [21]. Moreover, when considering time dependent correlations, this procedure leads to Gibbs potential which requires a proper renormalisation in order to be related to a Markov chain (see section 2.3.6).
- (ii) The Gibbs distributions considered by these approaches, with the naive form " $\frac{1}{Z}e^{-\beta H}$ ", where Z is a constant (while it depends on boundary terms in the general case) have a limited degree of application; in particular they do not extend easily to time dependent sequences with long memory, as spikes train emitted from neural networks might well be. Especially, considering already one time step Markov processes leads to substantial complications a shown in [44]. The "partition function" is not a constant (see eq. (1) of paper [44]) and needs to be approximated (eq. (4) of the same paper) using the (unproved) assumption of detailed balance, which is moreover a sufficient but non necessary condition for the existence of an equilibrium state, and may hardly generalize to more elaborated models.
- (iii) It does not allow to treat in a straightforward way the time-evolution of the Gibbs distribution (e.g. induced by mechanisms such as synaptic plasticity).

However, more general forms of Gibbs distributions have been introduced since long [74, 64, 5], in a theory called "thermodynamic formalism" introduced in the realm of dynamical systems and ergodic theory, allowing to treat infinite time sequences of processes with long (and even infinite [43]) memory. In this paper, we use the thermodynamic formalism to propose a generalisation of the existing models used for spike

trains statistics analysis which results in a more powerful framework that overcomes some of the weaknesses mentioned above. Our results are grounded on well established theoretical basements (see e.g. [38]) completed by recent results of the authors dealing with collective spike trains statistics in neural *networks* models [12, 11]. The theoretical framework of our approach is presented in the section 2. We propose a global approach to spike train analysis, going beyond the usual approaches essentially because it allows us to take into account (long term) *memory effects* in dynamics (sections 2.1,2.2). As a matter of fact we deal with models considering *spatio-temporal* and time-*causal* structure of spike trains emitted by neural networks together with the fact that some spike sequences (or “words”) might be forbidden by dynamics, introducing the notion of *grammar*. We propose a spectral method which provides directly the “free energy density” and the Kullback-Leibler divergence between the empirical statistics and the statistical model (section 2.3). This method does not assume a specific potential form and allows us to handle correctly non-normalized potentials. It does not require the assumption of detailed balance (necessary to apply Markov Chain Monte-Carlo (MCMC) methods) and offers a control of finite-size sampling effects, inherent to empirical statistics, by using large deviations results (Section 2.4). The price to pay is to introduce a somewhat heavy, but necessary, mathematical formalism. In several places we make connections with existing methods to clarify these concepts.

These theoretical basements allows us to propose, in section 3, a numerical method to parametrically estimate, and possibly compare, models for the statistics of simulated multi-cell-spike trains. Our method is not limited to firing rates models, pairwise synchronizations as [66, 73, 72] or 1-step time pairwise correlations models as [44], but deals with general form of Gibbs distributions, with parametric potentials corresponding to a spike n -uplets expansion, with multi-units and multi-times terms. The method is exact (in the sense that it does not involve heuristic minimization techniques). Moreover, we perform fast and reliable estimate of quantities such as the Kullback-Leibler divergence allowing a comparison between different models, as well as the computation of standard statistical indicators, and a further analysis about convergence rate of the empirical estimation and large deviations.

In section 4 we perform a large battery of tests allowing us to experimentally validate the method. First, we analyse the numerical precision of parameter estimation. Second, we generate synthetic data with a given statistics, and compare the estimation obtained using these data for several models. Moreover, we simulate a neural network and propose the estimation of the underlying Gibbs distribution parameters whose analytic form is known [11]. We also perform the estimation for several models using data obtained from a simulated neural network with stationary dynamics after Spike-Time dependent synaptic plasticity. Finally, we show results on the parameters estimation from synthetic data generated by a non-stationary statistical model.

2 Spike trains statistics from a theoretical perspective.

2.1 General context

2.1.1 Neural network dynamics.

We consider the evolution of a network of N neurons, described by a dynamical model, that is, either a deterministic dynamical system or a stochastic dynamical system (usually governed by both a deterministic evolution map and additive noise). We assume that there is a minimal time scale δ , set to $\delta = 1$ without loss of generality, at which dynamics can be time-discretized. Typically, this can be the minimal resolution of the spike time, constrained by biophysics and by measurements methods (see [9] for a discussion on time discretisation in spiking neural networks). The typical neuron models we think of are punctual conductance based generalized Integrate-and-Fire (IF) models with exponential synapses (gIF) [13]. Actually, the formalism developed here has been rigorously founded in [11] for Leaky-Integrate-and-Fire (LIF) models with noise. We further assume the network parameters (synaptic weights, currents, etc..) to be fixed in this context (see [13] for a discussion). This means that we assume observing a period of time where the system parameters are essentially constants. In other words, we focus here on *stationary* dynamics. This restriction is further discussed in section 4.3.5.

We are interested in situations where neurons dynamics, and especially spikes occurrences, do not show any regularity or exact reproducibility and require a statistical treatment. This is obviously the case for stochastic evolutions but this also happens in the deterministic case, whenever dynamics exhibits initial conditions sensitivity. This leads us to the choice of the statistical formalism proposed here, called the “thermodynamic formalism¹” (see [12] for an extended discussion).

2.1.2 Dynamics and raster plots.

Each neuron of index $i = 0 \dots N - 1$ is characterized by its state, X_i , which belongs to some (bounded) set $\mathcal{S} \in \mathbb{R}^M$. M is the number of variables characterizing the state of one neuron (we assume that all neurons are described by the same number of variables). A typical example is $M = 1$ where $X_i = V_i$ is the membrane potential of neuron i and $\mathcal{S} = [V_{min}, V_{max}]$ but the present formalism affords extensions to such additional characteristics as activation variables (e.g. for the Hodgkin-Huxley model [31] $M = 4$). The variable $X = [X_i]_{i=0}^{N-1}$ represents the state of a network of N neurons. Without loss of generality, we assume that all neurons have the same properties so that $X \in \mathcal{M} = \mathcal{S}^N$, where \mathcal{M} is the phase space where dynamics occurs. The evolution of the network over an infinite time is characterized by a *trajectory* $\tilde{X} \stackrel{\text{def}}{=} \{X(t)\}_{t=-\infty}^{+\infty}$.

One can associate to each neuron i a variable $\omega_i(t) = 1$ if neuron i fires between $[t, t + 1[$ and $\omega_i(t) = 0$ otherwise. A “spiking pattern” is a vector $\omega(t) \stackrel{\text{def}}{=} [\omega_i(t)]_{i=0}^N - 1$

¹This terminology has been introduced by Sinai [74], Ruelle [64] and Bowen [5] because of its analogy with statistical physics. But it does not relies on the principles of thermodynamics. Especially, the maximization of statistical entropy, discussed below, does not requires the invocation of the second principle of thermodynamics.

which tells us which neurons are firing at time t . In this setting, a “raster plot” is a sequence $\omega \stackrel{\text{def}}{=} \{\omega(t)\}_{t=-\infty}^{+\infty}$, of spiking patterns. Finally a *spike block* is a finite set of spiking pattern, written:

$$[\omega]_{t_1}^{t_2} = \{\omega(t)\}_{\{t_1 \leq t \leq t_2\}},$$

where spike times have been prescribed between the times t_1 to t_2 .

To each trajectory $\tilde{X} = \{X(t)\}_{t=-\infty}^{+\infty}$ is associated a raster plot $\omega = \{\omega(t)\}_{t=-\infty}^{+\infty}$. This is the sequence of spiking patterns displayed by the neural network when it follows the trajectory \tilde{X} . We write $\tilde{X} \rightarrow \omega$. On the other way round, we say that an infinite sequence $\omega = \{\omega(t)\}_{t=-\infty}^{+\infty}$ is an *admissible raster plot* if dynamics allows a trajectory \tilde{X} such that $\tilde{X} \rightarrow \omega$. We call Σ the set of admissible raster plots. The dynamics of the neurons state induces therefore a dynamics on the set of admissible raster plots, represented by the *left shift*, σ , such that $\sigma\omega = \omega' \Leftrightarrow \omega'(t) = \omega(t+1), \forall t \geq 0$. Thus, in some sense, raster plots provide a code for the trajectories \tilde{X} . Note that the correspondence may not be one-to-one [10].

Though dynamics produces many possible raster plots, it is important to remark that it is not able to produce *any* possible sequence of spiking patterns. This depends on the system properties (e.g., refractoriness forbids raster plots with spike interval below $1ms$) and parameters (e.g., after synaptic weight adaptation the dynamics often appears more constrained). For example, inhibition may prevent a neuron to fire whenever a group of pre-synaptic neurons has fired before. There are therefore *allowed* and *forbidden* sequences, constrained by dynamics. This corresponds to the following *crucial* property, often neglected in entropy estimations of spike trains [59]. The set of admissible raster plot Σ is *not the set of all possible raster plots*. Indeed, considering spike blocks of size n there are 2^{2^n} possible spike blocks but quite a bit less *admissible* raster plots (the exponential rate of growths in the number of admissible raster plots is given by the topological entropy which is an upper bound for the Kolmogorov-Sinai entropy defined in eq. (3), footnote 6).

2.1.3 Transition probabilities.

Typically, the network dynamics and the related spikes fluctuate in an unpredictable manner. The spike response itself is not sought as a deterministic response in this context, but as a conditional probability [59]. “Reading out the code” consists of inferring such probability. Especially, the probability that a neuron emits a spike at some time t depends on the history of the neural network. However, it is impossible to know explicitly its form in the general case since it depends on the past evolution of all variables determining the neural network state \mathbf{X} . A possible simplification is to consider that this probability depends *only* on the spikes emitted in the past by the network. In this way, we are seeking a family of transition probabilities of the form $P[\omega(t) | [\omega]_{-\infty}^{t-1}]$ from which all spike trains statistical properties can be deduced. These transition probabilities are called *conditional intensity* in [35, 7, 18, 36, 82, 51, 81, 56] and they are essential to determine completely the spike trains statistics. The price to pay is that we have to consider processes with memory (which is not so shocking when dealing with neural networks).

These transition probabilities are unknown for most models but an explicit computation can be rigorously achieved in the case of a discrete time Leaky Integrate-and-Fire (LIF) neural networks with noise, in the stationary case (e.g. time independent stimulus) (see eq. (40) and [11]). Stationarity means here that the transition probability does not depend explicitly on t so that one can focus on transition probabilities of the form $P[\omega(0) | [\omega]_{-\infty}^{-1}]$ and infer the probability of any spike block by the classical Chapman-Kolmogorov equation [27]. To our knowledge this is the only example where the complete spike trains statistics can be rigorously and analytically computed. Note that the transition probability depends on a *unbounded* past in the LIF model. Indeed, the state of a neuron is reset whenever it fires, so the probability of a given spiking pattern at time 0 depends on the past up to a time when each neuron has fired at least once. However, this time cannot be bounded (though the probability that it is larger than some τ decays exponentially fast with τ) [11].

2.1.4 Gibbs distribution.

As far as the present paper is concerned, the main result in [11] states that some neural networks models *do have Gibbs distributions*, though of a quite more complex form than currently used in the literature. More precisely it is rigorously proved in [11] that in discrete-time LIF models² with noise the statistics of spike trains is characterized by a *Gibbs distribution* which is also an *equilibrium state*, where the potential can be *explicitly computed*, but *has infinite range*.

Let us be more explicit. Since we are using the terms “Gibbs distribution” and “equilibrium state” in a more general sense than the definition used in the neuroscience community for spike train statistics analysis, we give here the definition of these two terms. In several places in the paper we show the link between this formalism and the usual form, and explain why we need to use the present formalism for spike train analysis. The main difference is that we consider probability distributions on a set of spatio-temporal sequences where the “space” is the network, and where *time is infinite* so that the spike train probability distributions is defined on infinite time sequences³. This is the natural context when considering transition probabilities as introduced in the previous section. The price to pay is a more complex formulation than the classical $\frac{1}{Z} \exp(-\beta H)$, but the reward is having a formalism allowing us to handle spike trains statistics including memory terms, and an explicit way to compute the free energy density and the Kullback-Leibler divergence between the empirical statistics and a statistical model, as developed in the rest of the paper.

A probability distribution μ_ϕ on the set of *infinite* spike sequences Σ (raster plots) is a Gibbs distribution if there exists a function⁴ $\phi : \Sigma \rightarrow \mathbb{R}$, called a *potential*, such

²Without restriction on the synaptic weights except that they are finite.

³This corresponds to the “thermodynamic limit” in statistical physics but in our case thermodynamic limit means “time tends to infinity” instead of “dimension of the system tends to infinity”. As a matter of fact the number of neurons, N , is fixed and finite in the whole paper.

⁴Some regularity conditions, associated with a sufficiently fast decay of the potential at infinity, are also required, that we do not state here [38].

that the probability of a spike block $[\omega]_t^{t+n}$, for any $-\infty < t < +\infty$, and $n > 0$, obeys:

$$c_1 \leq \frac{\mu_\phi([\omega]_t^{t+n})}{\exp[-(n+1)P(\phi) + \sum_{k=t}^{t+n} \phi(\sigma^k \omega)]} \leq c_2, \quad (1)$$

where $P(\phi), c_1, c_2$ are some constants with $0 < c_1 \leq 1 \leq c_2$. Recall that σ is the shift on rasters defined in section 2.1.2. Basically, this expresses that, as n becomes large, $\mu_\phi([\omega]_t^{t+n})$ behaves⁵ like $\frac{\exp[\sum_{k=t}^{t+n} \phi(\sigma^k \omega)]}{\exp[(n+1)P(\phi)]}$.

An *equilibrium state* is a probability distribution μ_ϕ which satisfies the following variational principle:

$$P(\phi) \stackrel{\text{def}}{=} h(\mu_\phi) + \mu_\phi(\phi) = \sup_{\mu \in m^{(inv)}(\Sigma)} h(\mu) + \mu(\phi), \quad (2)$$

where $m^{(inv)}(\Sigma)$ is the set of invariant probability measures on Σ , $h(\mu)$ is the entropy⁶ of the probability μ , and $\mu(\phi) \stackrel{\text{def}}{=} \int \phi d\mu$ is the average of ϕ with respect to the probability μ . Note that the notion of Gibbs distribution and equilibrium state are not equivalent in general [38], but in the present context, they are [11].

The term $P(\phi)$, called the *topological pressure* in this context, is the formal analog of a thermodynamic potential (free energy density). It is a generating function for the cumulants of ϕ (see section 2.2.3 for explicit examples).

2.1.5 Gibbs potential.

In the case of discrete-time LIF models the potential ϕ is the log of the probability transition $P[\omega(t) | [\omega]_{-\infty}^{t-1}]$ [11]. We believe that this statement extends to more general situations: if a spike train is characterized by a Gibbs distribution then a natural candidate for the Gibbs potential is the log of the conditional intensity. Let us insist on this result. Beyond the mathematical intricacies grounding this statement, this choice is natural because it provides a (time) *causal* potential with *memory*. As a consequence, the statistics of spikes at a given time are causally related to the past spikes. This corresponds to potential having a *range* that can be large. A potential has range R if $\phi([\omega]_{-\infty}^0) = \phi([\omega]_{-(R-1)}^0)$. In terms of the transition probability, this corresponds to a system with a memory depth $R - 1$ (the probability that a neuron spike at time t

⁵In the sense of (1). Thus, "behaves like" does not mean "is equal to".

⁶The Kolmogorov-Sinai entropy or entropy rate of a probability μ is:

$$h[\mu] = \lim_{n \rightarrow +\infty} \frac{h^{(n)}[\mu]}{n}, \quad (3)$$

where

$$h^{(n)}[\mu] = - \sum_{\omega \in \Sigma^{(n)}} \mu([\omega]_0^{n-1}) \log \mu([\omega]_0^{n-1}), \quad (4)$$

$\Sigma^{(n)}$ being the set of admissible sequences of length n . This quantity provides the exponential rate of growth of admissible blocks having a positive probability under μ , as n grows. It is positive for chaotic system and it is zero for periodic systems.

depends on the spikes emitted by the network, up to time $t - (R - 1)$ back in the past⁷. Unfortunately even if the simplest known example of neural network model, the LIF, the range is (mathematically) infinite⁸. Is the situation simpler for more complex neural networks models, for real neural networks ? Fortunately, finite range approximations can be proposed, with a good control on the degree of approximation, as we now develop.

2.2 Markov approximations.

In the sequel, we make the assumption that the spike trains statistics of the system that we are observing is described by a Gibbs distribution whose potential has to be determined from empirical data.

2.2.1 Range- R potential.

It is always possible to propose Markov approximations of ϕ , even in the case where the Gibbs potential depends on spike sequences with unbounded length. This is the strategy that we now develop. We approximate the exact transition probability by a transition probability with finite memory of depth $R - 1$, $P[\omega(0) | [\omega]_{-(R-1)}^{-1}]$. In this context, as shown in [11], the exact Gibbs potential can be approximated⁹ by a *range- R potential* with a parametric form:

$$\psi(\omega) = \sum_{l=1}^R \sum_{(i_1, t_1), \dots, (i_l, t_l) \in \mathcal{P}(N, R)} \lambda_{i_1, n_{i_1}, \dots, i_l, n_{i_l}}^{(l)} \omega_{i_1}(n_{i_1}) \dots \omega_{i_l}(n_{i_l}). \quad (5)$$

This form is nothing but a Taylor expansion of $\log(P[\omega(0) | [\omega]_{-(R-1)}^{-1}])$, where one collects all terms of form $\omega_{i_1}^{k_1}(n_{i_1}) \dots \omega_{i_l}^{k_l}(n_{i_l})$, for integer k_1, \dots, k_l 's, using that $\omega_i^k(n) = \omega_i(n)$, for any $k > 0$ and any i, n . Here $\mathcal{P}(N, R)$ is the set of non repeated pairs of integers (i, n) with $i \in \{0, \dots, N - 1\}$ and $n \in \{0, \dots, R - 1\}$.

Such form of potential is a linear combination of *monomials*. An *order- n monomial* is a product $\omega_{i_1}(t_1) \dots \omega_{i_n}(t_n)$, where $0 \leq i_1 \leq i_2 \leq \dots \leq i_n \leq N - 1$, $0 \leq t_1 \leq t_2 \leq \dots \leq t_n < \infty$ and such that there is no repeated pair (i_k, t_k) , $k = 1 \dots n$. The monomial $\omega_{i_1}(t_1) \dots \omega_{i_n}(t_n)$ takes values in $\{0, 1\}$ and is 1 if and only if each neuron i_l fires at time t_l , $l = 1 \dots n$. On phenomenological grounds the monomial $\omega_{i_1}(t_1) \dots \omega_{i_n}(t_n)$ corresponds to a spike n -uplet $(i_1, t_1), \dots, (i_n, t_n)$ (neuron i_1 fires at time t_1 , neuron i_2 at time t_2 , etc ...).

2.2.2 Further approximations.

The potential (5) remains quite cumbersome since the number of terms in (6) explodes combinatorially as N, R growth. Equivalently, in terms of the classical Jaynes approach

⁷Hence range 1 or equivalently memory depth 0 means time independent events.

⁸Though the variation of ϕ decays exponentially fast ensuring the existence of a thermodynamic limit.

⁹In the case of LIF models the Kullback-Leibler divergence between the exact Gibbs distribution and its approximation by the potential (5) decays exponentially fast with R .

where the Gibbs distribution is obtained via the maximisation of statistical entropy under constraints (see section 2.4.3), one has to fix a number of constraints that grows exponentially fast with N, R . As a consequence, one is typically lead to consider parametric forms where monomials have been removed (or, sometimes, added) in the expansion. This constitutes a coarser approximation to the exact potential, but more tractable from the numerical or empirical point of view. To alleviate notations we write, in the rest of paper, the parametric potential in the form:

$$\psi = \sum_{l=1}^L \lambda_l \phi_l, \quad (6)$$

where ϕ_l 's are monomials. The choice of the parametric form defines what we call a “statistical model”, namely a Gibbs distribution, denoted μ_ψ in the sequel, for the potential (6). The question is “how far is this distribution from the true statistics” ?

2.2.3 Examples of range- R potentials

Bernoulli potentials The easiest example of potential are range-1 potentials (memoryless) where $\psi(\omega) = \sum_{i=0}^{N-1} \lambda_i \omega_i(0)$. The corresponding Gibbs distribution provides a statistical model where neurons are independent.

“Ising” like potentials. This type of potential has been introduced by Schneidman and collaborators in [67]. It reads, in our notations,

$$\psi(\omega) = \sum_{i=0}^{N-1} \lambda_i \omega_i(0) + \sum_{i=0}^{N-1} \sum_{j=0}^{i-1} \lambda_{ij} \omega_i(0) \omega_j(0). \quad (7)$$

The corresponding Gibbs distribution provides a statistical model where synchronous pairwise correlations between neurons are taken into account, but neither higher order spatial correlations nor other time correlations are taken into account. As a consequence, the corresponding “Markov chain” is memoryless.

Pairwise Time-Dependent- k potentials with rates (RPTD- k).

An easy generalization of (7) is:

$$\psi(\omega) = \sum_{i=0}^{N-1} \lambda_i \omega_i(0) + \sum_{i=0}^{N-1} \sum_{j=0}^{i-1} \sum_{\tau=-k}^k \lambda_{ij\tau} \omega_i(0) \omega_j(\tau), \quad (8)$$

called *Pairwise Time-Dependent k (RPTD- k) with Rates* potentials in the sequel.

Pairwise Time-Dependent k (PTD- k) potentials.

A variation of (8) is to avoid the explicit constraints associated to firing rates :

$$\sum_{i=0}^{N-1} \sum_{j=0}^{i-1} \sum_{\tau=-k}^k \lambda_{ij\tau} \omega_i(0) \omega_j(\tau), \quad (9)$$

called **Pairwise Time-Dependent k (PTD- k)** potentials in the sequel.

2.2.4 Encoding spike blocks

To each spike block of length R , $[\omega]_k^{k+R-1}$, $k \in \mathbb{Z}$, one can associate an integer:

$$w_k = \sum_{t=k}^{k+R-1} \sum_{i=0}^{N-1} 2^{i+Nt} \omega_t(t). \quad (10)$$

One has 2^{NR} such possible blocks (though some of them can be forbidden by dynamics).

We use the following notation:

$$\sigma w_k = \sum_{t=k+1}^{k+R} \sum_{i=0}^{N-1} 2^{i+Nt} \omega_t(t), \quad (11)$$

so that, w_k represents the block $[\omega]_k^{k+R-1}$ and $\sigma w_k = w_{k+1}$ represents the block $[\omega]_{k+1}^{k+R}$.

In this setting a range- R potential is therefore a vector in the space $\mathcal{H} \stackrel{\text{def}}{=} \mathbb{R}^{2^{NR}}$ with components $\psi_w \stackrel{\text{def}}{=} \psi(\omega)$. This amounts to recoding spiking sequences as sequences of spike blocks of length R , associated with words w_k , taking into account the memory depth of the Markov chain.

2.3 Determining the statistical properties of a Gibbs distribution.

We now introduce the thermodynamic formalism allowing us to compute numerically the main statistical properties of a Gibbs distribution. This approach is different from a classical approach in statistical physics where one tries to compute the partition function. The present approach gives directly the topological pressure (corresponding to the free energy density in the thermodynamic limit) from which the statistical properties can be inferred.

2.3.1 The Ruelle-Perron-Frobenius operator.

Once the parametric form of the potential is given, the statistical properties of the Gibbs distribution are obtained by the Ruelle-Perron-Frobenius (RPF) operator introduced by Ruelle in [62]. In the present case this is a positive $2^{NR} \times 2^{NR}$ matrix, $L(\psi)$, with entries

$$L_{w',w}(\psi) = e^{\psi_{w'}} G_{w',w}, \quad (12)$$

(while it acts on functional spaces in the infinite range case).

The matrix G is called the *grammar*. It encodes in its definition the *essential fact* that the underlying dynamics is not able to produce all possible raster plots:

$$G_{w',w} = \begin{cases} 1, & \text{if the transition } w' \rightarrow w \text{ is admissible;} \\ 0, & \text{otherwise.} \end{cases} \quad (13)$$

Since we are considering blocks of the form¹⁰ $w' \sim [\omega]_k^{k+R-1} = \omega(k) \dots \omega(k+R-$

¹⁰Since dynamics is assumed stationary the result actually does not depend on k .

1) and $w \sim [\omega]_{k+1}^{k-R} = \omega(k+1) \dots \omega(k-R)$, the transition $w' \rightarrow w$ is legal if¹¹ w' and w have the spiking patterns $\omega(k+1) \dots \omega(k+R-1)$ in common. Thus, while there are 2^{NR} blocks for a network of N neurons, the matrix G has at most 2^N non zero entries on each line. As a consequence $L(\psi)$ is *sparse*.

Note also that all non zeroes entries $L_{w',w}(\psi)$ on a given line are equal. This degeneracy comes from our choice to represent ψ as a vector in \mathcal{H} which is the easiest for numerical purposes. This has consequences discussed in the section 2.3.6.

2.3.2 The Ruelle-Perron-Frobenius theorem

In the present paper we make the assumption that the underlying (and hidden) dynamics is such that the $L(\psi)$ matrix is primitive, i.e. $\exists n > 0$, s.t. $\forall w, w' L_{w',w}^n(\psi) > 0$. This assumption holds for Integrate-and-Fire models with noise and is likely to hold for more general neural networks models where noise renders dynamics ergodic and mixing [11]. Note, on the opposite, that if this assumption is not fulfilled there are little chances to characterize spike trains statistics with a (unique) Gibbs distribution.

Then, $L(\psi)$ obeys the Perron-Frobenius theorem¹²:

Theorem 1 $L(\psi)$ has a unique maximal and strictly positive eigenvalue $s(\psi) = e^{P(\psi)}$ associated with a right eigenvector $\mathbf{b}(\psi)$ and a left eigenvector $\langle \mathbf{b}(\psi)$, with positive and bounded entries, such that $L(\psi)\mathbf{b}(\psi) = s(\psi)\mathbf{b}(\psi)$, $\langle \mathbf{b}(\psi)L(\psi) = s(\psi)\langle \mathbf{b}(\psi)$. Those vectors can be chosen such that $\langle \mathbf{b}(\psi) \cdot \mathbf{b}(\psi) \rangle = 1$ where \cdot is the scalar product in \mathcal{H} . The remaining part of the spectrum is located in a disk in the complex plane, of radius strictly lower than $s(\psi)$. As a consequence, for all \mathbf{v} in \mathcal{H} ,

$$\frac{1}{s(\psi)^n} L^n(\psi)\mathbf{v} \rightarrow \mathbf{b}(\psi)\langle \mathbf{b}(\psi) \cdot \mathbf{v} \rangle, \quad (14)$$

as $n \rightarrow \infty$.

The Gibbs-probability of a spike block w of length R is

$$\mu_\psi(w) = b_w(\psi)\langle b_w(\psi) \rangle, \quad (15)$$

where $b_w(\psi)$ is the w -th component of $\mathbf{b}(\psi)$.

As a consequence, the assumption of primitivity guarantees the existence and uniqueness of a Gibbs distribution. Note that it is more general than the detailed balance assumption.

2.3.3 Computing averages of monomials

Since $\mu_\psi[\phi_l] = \sum_w \mu_\psi[w]\phi_l(w)$ one obtains using (15):

$$\mu_\psi[\phi_l] = \sum_{w \in \mathcal{H}} b_w(\psi)\phi_l(w)\langle b_w(\psi) \rangle. \quad (16)$$

This provides a fast way to compute $\mu_\psi[\phi_l]$.

¹¹Additional transitions are usually forbidden by dynamics. As a consequence, those transitions have a zero probability of occurrence and they can be detected on empirical sequences (see section 3.4.1).

¹²This theorem has been generalized by Ruelle to infinite range potentials under some regularity conditions [63, 64].

2.3.4 The topological pressure.

The RPF theorem gives a direct access to the topological pressure $P(\psi)$ which is the logarithm of the leading eigenvalue $s(\psi)$, easily obtained by a power method (see eq. (14)). In the case of range- R potentials (6) where the topological pressure $P(\psi)$ becomes a function of the parameters $\lambda = (\lambda_l)_{l=1}^L$, we write $P(\lambda)$. One can show that the topological pressure is the generating function for the cumulants of the monomials ϕ_l :

$$\frac{\partial P(\lambda)}{\partial \lambda_l} = \mu_\psi[\phi_l]. \quad (17)$$

Higher order cumulants are obtained likewise by successive derivations. Especially, second order moments related to the central limit theorem obeyed by Gibbs distributions [5, 38] are obtained by second order derivatives. As a consequence of this last property, the topological pressure's Hessian is positive and the topological pressure is *convex* with respect to λ .

2.3.5 Entropy

Since μ_ψ is a Gibbs distribution, for the potential ψ , therefore, an exact expression for the Kolmogorov-Sinai entropy (3) can be readily obtained:

$$h[\mu_\psi] = P(\lambda) - \sum_l \lambda_l \mu_\psi[\phi_l]. \quad (18)$$

2.3.6 Normalisation

When switching from the potential (5), which is the polynomial expansion of the log of the conditional intensity, to a simplified parametric form (6), one introduces several biases. First, one may add terms which are not in the original potential. Second, (5) must satisfy a constraint corresponding to the fact that $\psi(\omega)$ is the log of a probability. Such a potential is called *normalized*. Its main characteristics are (i) the topological pressure is zero; (ii) the right eigenvector $\mathbf{b}(\psi)$ has all its components equal. The reason is simple: when the potential is the log of a transition probability the RPF operator satisfies $\sum_{w' \in \mathcal{H}} L_{w'w} = \sum_{\omega(0) \in \{0,1\}^N} P[\omega(0) | [\omega]_{-(R-1)}^{-1}] = 1, \forall w' \in \mathcal{H}$, where w' corresponds e.g. to $[\omega]_{-R}^{-1}$, and w to $[\omega]_{-(R-1)}^0$. Thus, the largest eigenvalue $s(\psi)$ is 1, and the corresponding right eigenvector has all its components equal.

On the opposite, the parametric form (6) where λ_l are free parameters is in general *not normalized*, with deep consequences discussed in the next sections. However, there exists a transformation allowing to convert an arbitrary range- R potential to a normalized potential Ψ by the transformation:

$$\Psi_{w'w} = \psi_{w'w} - \log(b_{w'}(\psi)) + \log(b_w(\psi)) - P(\psi). \quad (19)$$

Let us give two examples. First, if ψ is normalized then $b_{w'}(\psi) = b_w(\psi)$ and $P(\psi) = 0$ so that (fortunately) $\Psi = \psi$. Second, if ψ has range-1 then, according to the computations done in section 2.3.8, $\Psi_{w'w} = -\log(Z) + \psi_{w'w} = -\log(Z) + \psi(\omega(0))$.

Here, the normalisation only consists of removing the log of a (constant) partition function.

In the general case, the potential (19) has range- $R + 1$. The corresponding RPF operator $L(\Psi)$, is therefore the transition matrix for a R -step Markov chain. Thus, switching to a parametric form (6) without constraint on the λ_i 's we end up with a redundant transition probability of form $P'(\omega(0) | [\omega]_{-R}^{-1})$ while the right transition probability is $P(\omega(0) | [\omega]_{-(R-1)}^{-1})$. Since, obviously $P'(\omega(0) | [\omega]_{-R}^{-1}) = P(\omega(0) | [\omega]_{-(R-1)}^{-1})$ the final form of the normalized potential can be easily simplified.

2.3.7 Probability of arbitrary spike blocks

Using the normalized potential (19) the probability of a *admissible* spike block of size strictly larger than R , $[\omega]_t^{t+n+R-1}$, $t \in \mathbb{Z}$, $n > 0$ is given by:

$$\mu_\Psi \left[[\omega]_t^{t+n+R-1} \right] = \mu_\Psi [\omega(t), \omega(t+1) \dots \omega(t+n+R-1)] = \mu_\Psi [w_t, \dots, w_{t+n}],$$

where the word w_k encodes the block $[\omega]_k^{k+R-1}$. As a consequence,

$$\mu_\Psi [w_t, \dots, w_{t+n}] = \mu_\Psi [w_t] L_{w_t, w_{t+1}}(\Psi) L_{w_{t+1}, w_{t+2}}(\Psi) \dots L_{w_{t+n-1}, w_{t+n}}(\Psi). \quad (20)$$

This is the classical Chapman-Kolmogorov equation. Returning to the initial (non-normalised) potential (6) this relation reads, using (19):

$$\mu_\Psi [w_t, \dots, w_{t+n}] = \mu_\Psi [w_t] \frac{b_{w_{t+n}}(\Psi)}{b_{w_t}(\Psi)} \frac{1}{e^{(n+1)P(\Psi)}} e^{\sum_{k=t}^{t+n} \Psi_{w_k}}. \quad (21)$$

One checks¹³ that $\mu_\Psi [w_t, \dots, w_{t+n}]$ satisfies the definition of a Gibbs distribution (1) with $P(\Psi) = \log s(\Psi)$ and $w_k = \sigma^k w_0$.

On the opposite, for blocks of size $0 < n < R + 1$ then

$$\mu_\Psi \left[[\omega]_t^{t+n} \right] = \sum_{w \subset [\omega]_t^{t+n}} \mu_\Psi(w),$$

where the sum holds on each word w containing the block $[\omega]_t^{t+n}$.

2.3.8 Links with the simple Gibbs form.

In this section we make the link between our formalism and previous approaches using the simple Gibbs formulation.

As a preliminary remark note that the Gibbs-probability of a spike block w of length R , given by (15), *hasn't* the form $\frac{1}{Z} e^{\Psi(w)}$, with Z constant, *except when* $R = 1$. The case $R = 1$ corresponds to a Markov chain without memory, where therefore the spiking pattern $w_t = \omega(t)$ is independent on $w_{t-1} = \omega(t-1)$. Examples are the Bernoulli model (where moreover spikes are spatially independent) or the Ising model (where spikes are spatially correlated but not time correlated). In this case, all transitions

¹³Taking into account the fact that symbols w_k encode spike blocks of length R .

are allowed, thus the RPF matrix reads $L_{w',w}(\psi) = e^{\psi_{w'}}$ and does not depend on w . As a consequence, all lines are linearly dependent which implies that there are $N - 1$ 0-eigenvalues while the largest eigenvalue is $Z \stackrel{\text{def}}{=} s(\psi) = \text{Tr}(L(\psi)) = \sum_{w' \in \mathcal{H}} e^{\psi_{w'}}$.

The corresponding left eigenvector is $\langle \mathbf{b}(\psi) = (1, \dots, 1)$ and the right eigenvector is $b_{w'}(\psi) = \frac{e^{\psi_{w'}}}{Z}$, so that $\langle \mathbf{b}(\psi), \mathbf{b}(\psi) \rangle = 1$. Thus, the Gibbs distribution is, according to (15), $\mu_{w'} = \frac{e^{\psi_{w'}}}{Z}$.

Consider now larger ranges. Recall first that a potential of form (6) is in general not normalized. To associate it to a Markov chain one has to use the transformation (19) and the probability of a spiking pattern sequence is given by (21). In particular, the joint probability of two admissible successive blocks w', w reads $\mu_{\psi}(w, w') = \mu_{\psi}[w'] \frac{b_w(\psi)}{b_{w'}(\psi)} \frac{1}{e^{P(\psi)}} e^{\psi_{ww'}}$. One can introduce a formal Hamiltonian $H_{ww'} = \psi_{ww'} + \log(b_w(\psi))$ and a “conditional” partition function $Z(w') = e^{P(\psi)} b_{w'}(\psi)$ such that $\mu_{\psi}(w|w') = \frac{1}{Z(w')} e^{H_{ww'}}$ with $Z(w') = \sum_{w \in \mathcal{H}} e^{H_{ww'}}$ but here the partition function depends on w' (compare with eq. (1) in ref [44]). This corresponds, in statistical mechanics, to have interactions with a boundary. In this setting, the free energy density (topological pressure) is obtained (away from phase transitions¹⁴), via $\frac{1}{n} \log Z_n(w') \rightarrow P(\psi)$ as $n \rightarrow \infty$, $\forall w'$, requiring to consider a thermodynamic limit, as we do in the present setting.

As a conclusion, starting from an a priori form of a potential (6), obtained e.g. by Jaynes argument (see section 2.4.3) one obtains a non normalized potential which cannot be directly associated with a Markov chain, and the corresponding Gibbs measure hasn't the simple Gibbs form used for Ising model, as soon as one introduces memory terms in the potential. However, the thermodynamic formalism allows one to treat this case without approximations, or assumptions such as detailed balance, and gives direct access to the topological pressure.

2.3.9 Comparing several Gibbs statistical models.

The choice of a potential (6), i.e. the choice of a set of observables, fixes a statistical model for the statistics of spike trains. Clearly, there are many choices of potentials and one needs to propose a criterion to compare them. The Kullback-Leibler divergence,

$$d(\nu, \mu) = \limsup_{n \rightarrow \infty} \frac{1}{n} \sum_{[\omega]_0^{n-1}} \nu([\omega]_0^{n-1}) \log \left[\frac{\nu([\omega]_0^{n-1})}{\mu([\omega]_0^{n-1})} \right], \quad (22)$$

where ν and μ are two invariant probability measures, provides some notion of asymmetric “distance” between μ and ν .

The computation of $d(\nu, \mu)$ is delicate but, in the present context, the following holds. For ν an invariant measure and μ_{ψ} a Gibbs measure with a potential ψ , both defined on the same set of sequences Σ , one has [5, 63, 38, 16]:

$$d(\nu, \mu_{\psi}) = P(\psi) - \nu(\psi) - h(\nu). \quad (23)$$

¹⁴This requires a sufficiently fast decay of the potential, as mentioned in the footnote 4

This is the key of the algorithm that we have developed.

2.4 Computing the Gibbs distribution from empirical data.

2.4.1 Empirical Averaging

Assume now that we observe the spike trains generated by the neural network. We want to extract from these observations informations about the set of monomials ϕ_l constituting the potential and the corresponding coefficients λ_l .

Typically, one observes, from \mathcal{N} repetitions of the same experiment, i.e. submitting the system to the same conditions, \mathcal{N} raster plots $\omega^{(m)}, m = 1 \dots \mathcal{N}$ on a finite time horizon of length T . These are the basic data from which we want to extrapolate the Gibbs distribution. The key object for this is the *empirical* measure. For a fixed \mathcal{N} (number of observations) and a fixed T (time length of the observed spike train), the *empirical average* of a function $f : \Sigma \rightarrow \mathbb{R}$ is:

$$\bar{f}^{(\mathcal{N}, T)} = \frac{1}{\mathcal{N}T} \sum_{m=1}^{\mathcal{N}} \sum_{t=1}^T f(\sigma^t \omega^{(m)}). \quad (24)$$

Typical examples are $f(\omega) = \omega_i(0)$ in which case the empirical average of f is the firing rate¹⁵ of neuron i ; $f(\omega) = \omega_i(0)\omega_j(0)$ then the empirical average of f measures the estimated probability of spike coincidence for neuron j and i ; $f(\omega) = \omega_i(\tau)\omega_j(0)$ then the empirical average of f measures the estimated probability of the event “neuron j fires and neuron i fires τ time step later” (or sooner according to the sign of τ).

Note that in (24) we have used the shift σ^t for the time evolution of the raster plot. This notation is compact and well adapted to the next developments than the classical formula, reading, e.g., for firing rates $\frac{1}{\mathcal{N}T} \sum_{m=1}^{\mathcal{N}} \sum_{t=1}^T f(\omega^{(m)}(t))$.

The empirical measure is the probability distribution $\pi^{(T)}$ such that, for any function¹⁶ $f : \Sigma \rightarrow \mathbb{R}$,

$$\pi^{(T)}(f) = \bar{f}^{(\mathcal{N}, T)}. \quad (25)$$

Equivalently, the empirical probability of a spike block $[\omega]_{t_1}^{t_2}$ is given by:

$$\pi^{(T)}\left([\omega]_{t_1}^{t_2}\right) = \frac{1}{\mathcal{N}T} \sum_{m=1}^{\mathcal{N}} \sum_{t=1}^T \chi_{[\omega]_{t_1}^{t_2}}(\sigma^t \omega^{(m)}), \quad (26)$$

where $\chi_{[\omega]_{t_1}^{t_2}}$ is the indicatrix function of the block $[\omega]_{t_1}^{t_2}$ so that $\sum_{t=1}^T \chi_{[\omega]_{t_1}^{t_2}}(\sigma^t \omega^{(m)})$ simply counts the number of occurrences of the block $[\omega]_{t_1}^{t_2}$ in the empirical raster $\omega^{(m)}$.

2.4.2 Estimating the potential from empirical average

The empirical measure is what we get from experiments while it is assumed that spike statistics is governed by an hidden Gibbs distribution μ_ψ that we want to determine or approximate. Clearly there are infinitely many *a priori* choices for this distribution,

¹⁵Recall that we assume dynamics is stationary so rates do not depend on time.

¹⁶In fact, it is sufficient here to consider monomials.

corresponding to infinitely many a priori choices for the potential ψ . However, the ergodic theorem (the law of large number) states that $\pi^{(T)} \rightarrow \mu_\psi$ as $T \rightarrow \infty$ where μ_ψ is the sought Gibbs distribution. Equivalently, the Kullback-Leibler divergence $d(\pi^{(T)}, \mu_\psi)$ between the empirical measure and the sought Gibbs distribution *tends to 0* as $T \rightarrow \infty$.

Since we are dealing with finite samples the best that we can expect is to find a Gibbs distribution which *minimizes* this divergence. This is the core of our approach. Indeed, using eq. (23) we use the approximation¹⁷:

$$d(\pi^{(T)}, \mu_\psi) = P(\psi) - \pi^{(T)}(\psi) - h(\pi^{(T)}). \quad (27)$$

The advantage is that this quantity can be numerically estimated, since for a given choice of ψ the topological pressure is known from the Ruelle-Perron-Frobenius theorem, while $\pi^{(T)}(\psi)$ is directly computable. Since $\pi^{(T)}$ is fixed by the experimental raster plot, $h(\pi^{(T)})$ is independent of the Gibbs potential, so we can equivalently minimize:

$$\tilde{h}[\psi] = P[\psi] - \pi^{(T)}(\psi), \quad (28)$$

without computing the entropy $h(\pi^{(T)})$.

This relation holds for any potential. In the case of a parametric potential of the form (6) we have to minimize

$$\tilde{h}[\lambda] = P[\lambda] - \sum_{l=1}^L \lambda_l \pi^{(T)}(\phi_l). \quad (29)$$

Thus, from (17) and (24), given the parametric form, the set of λ_l 's minimizing the KL divergence are given by:

$$\mu_\psi[\phi_l] = \pi^{(T)}(\phi_l), \quad l = 1 \dots L. \quad (30)$$

Before showing why this necessary condition is also sufficient, we want to comment this result in connection with standard approaches (“Jaynes argument”).

2.4.3 Inferring statistics from empirical averages of observables: The Jaynes argument.

The conditions (30) impose constraints on the sought Gibbs distribution. In view of the variational principle (2) the minimization of KL divergence *for a prescribed parametric form of the Gibbs potential* is equivalent to *maximizing the statistical entropy under the constraints (30)*, where the λ_l 's appear as adjustable Lagrange multipliers. This is the Jaynes argument [34] commonly used to introduce Gibbs distributions in statistical physics textbooks, and also used in the fundating paper of Schneiderman et al. [67]. There is however an important subtlety that we want to outline. The Jaynes argument provides the Gibbs distribution which minimizes the KL divergence with respect to the empirical distribution *in a specific class of Gibbs potentials*. Given a parametric form for the potential it gives the set of λ_l 's which minimizes the KL divergence for the set

¹⁷This is an approximation because $\pi^{(T)}$ is not invariant [38]. It becomes exact as $T \rightarrow +\infty$.

of Gibbs measures having *this form of potential* [21]. Nevertheless, the divergence can still be quite large and the corresponding parametric form can provide a poor approximation of the sought measure. So, in principle one has to minimize the KL divergence with respect to several parametric forms. This is a way to compare the statistical models. The best one is the one which minimizes (29), i.e. knowing if the “model” ψ_2 is significantly “better” than ψ_1 , reduces to verifying:

$$\tilde{h}[\psi_2] \ll \tilde{h}[\psi_1], \quad (31)$$

easily computable at the implementation level, as developed below. Note that \tilde{h} has the dimension of entropy. Since we compare entropies, which units are bits of information, defined in base 2, the previous comparison units is well-defined.

2.4.4 Convexity.

The topological pressure is convex with respect to λ . As being the positive sum of two (non strictly) convex criteria $P[\psi]$ and $-\pi^{(T)}(\psi)$ in (29), the minimized criterion is convex. This means that the previous minimization method intrinsically converges towards a global minimum.

Let us now consider the estimation of an hidden potential $\psi = \sum_{l=1}^L \lambda_l \phi_l$ by a test potential $\psi^{(test)} = \sum_{l=1}^{L^{(test)}} \lambda_l^{(test)} \phi_l^{(test)}$. As a consequence, we estimate ψ with a set of parameters $\lambda_l^{(test)}$, and the criterion (29) is minimized with respect to *those parameters* $\lambda_l^{(test)}$, $l = 1 \dots L^{(test)}$.

Several situations are possible. First, ψ and $\psi^{(test)}$ have the same set of monomials, only the λ_l 's must be determined. Then, the unique minimum is reached for $\lambda_l^{(test)} = \lambda_l, l = 1 \dots L$. Second, $\psi^{(test)}$ contains all the monomials of ψ plus additional ones (*overestimation*). Then, the $\lambda_l^{(test)}$'s corresponding to monomials in ψ converge to λ_l while the coefficients corresponding to additional monomials converge to 0. The third case corresponds to *underestimation*. $\psi^{(test)}$ contains less monomials than ψ or distinct monomials. In this case, there is still a minimum for the criterion (29), but it provides a statistical model (a Gibbs distribution) at *positive KL distance* from the correct potential [21]. In this case adding monomials to $\psi^{(test)}$ will improve the estimation. More precisely, if for a first test potential the coefficients obtained after minimisation of \tilde{h} are $\lambda_l^{(test)}, l = 1 \dots L^{(test)}$ and for a second test potential they are $\lambda_l'^{(test)}, l = 1 \dots L'(test), L'(test) > L^{(test)}$ then $\tilde{h}(\lambda_1^{(test)}, \dots, \lambda_{L^{(test)}}^{(test)}) \geq \tilde{h}(\lambda_1'^{(test)}, \dots, \lambda_{L'(test)}'^{(test)})$. For the same l the coefficients $\lambda_l^{(test)}$ and $\lambda_l'^{(test)}$ can be quite different.

Note that these different situations are not inherent to our procedure, but to the principle of finding an hidden probability by maximizing the statistical entropy under constraints, when the full set of constraints is not known¹⁸. Examples of these cases are provided in section 4. As a matter of fact, we have therefore two strategies to

¹⁸The problem of estimating the memory order of the underlying markov chain to a given sequence, which means, in our framework, to find the the potential range, has been a well known difficult question in coding and information theory [49]. Some of the current available tests might offer additional algorithmic tools that would be explored in a forthcoming paper

estimate an hidden potential. Either starting from a minimal form of test potential (e.g. Bernoulli) and adding successive monomials (e.g. based on heuristical arguments such as “pairwise correlations do matter”) to reduce the value of \tilde{h} . The advantage is to start from potentials with a few number coefficients, but where the knowledge of the coefficients at a given step cannot be used at the next step, and where one has no idea on “how far” we are from the right measure. The other strategy consists of starting from the largest possible potential with range R ¹⁹. In this case it is guarantee that the test potential is at the minimal distance from the sought one, in the set of range- R potential, while the minimization will remove irrelevant monomials (their coefficient vanishes in the estimation). The drawback is that one has to start from a very huge number of monomials (2^{NR}) which reduces the number of situations one can numerically handle. These two approaches are used in section 4.

2.4.5 Finite sample effects and large deviations.

Note that the estimations crucially depend on T . This is a central problem, not inherent to our approach but to all statistical methods where one tries to extract statistical properties from finite empirical sample. Since T can be small in practical experiments, this problem can be circumvented by using an average over several samples (see eq. (24) and related comments). Nevertheless it is important to have an estimation of finite sampling effects, which can be addressed by the large deviations properties of Gibbs distributions.

For each observable ϕ_l , $l = 1 \dots L$, the following holds, as $T \rightarrow +\infty$ [22]:

$$\mu_\psi \left\{ \omega, |\pi^{(T)}(\phi_l) - \mu_\psi(\phi_l)| \geq \varepsilon \right\} \sim \exp(-TI_l(\varepsilon)), \quad (32)$$

where $I_l(x) = \sup_{\lambda_l \in \mathbb{R}} (\lambda_l x - P[\lambda])$, is the Legendre transform of the pressure $P[\lambda]$.

This result provides the convergence rate with respect to T . This is very important, since, once the Gibbs distribution is known, one can infer the length T of the time windows over which averages must be performed in order to obtain reliable statistics. This is of particular importance when applying statistical tests such as Neymann-Pearson for which large deviations results are available in the case of Markov chains and Gibbs distributions with finite range potentials [50].

Another important large deviation property also results from thermodynamic formalism [38, 14, 22]. Assume that the experimental raster plot ω is distributed according to the Gibbs distribution μ_ψ , with potential ψ , and assume that we propose, as a statistical model, a Gibbs distribution with potential $\psi' \neq \psi$. The Gibbs measure of spike blocks of range (15) is a vector in \mathcal{H} and $\pi^{(T)} = \left(\pi^{(T)}(w) \right)_{w \in \mathcal{H}}$ is a random vector. Now, the probability $\mu_\psi \left\{ \|\pi^{(T)} - \mu_{\psi'}\| < \varepsilon \right\}$ that $\pi^{(T)}$ is ε -close to the “wrong” probability $\mu_{\psi'}$ decays exponentially fast as,

$$\mu_\psi \left\{ \|\pi^{(T)} - \mu_{\psi'}\| < \varepsilon \right\} \sim \exp(-T \inf_{\mu, \|\mu - \mu_{\psi'}\| < \varepsilon} d(\mu, \mu_\psi)). \quad (33)$$

¹⁹ibid.

Thus, this probability decreases exponentially fast with T , with a rate given (for small ε) by $T d(\mu_\psi, \mu_{\psi'})$. Therefore, a difference of η in the Kullback-Leibler divergences $d(\pi^{(T)}, \mu_\psi)$, $d(\pi^{(T)}, \mu_{\psi'})$ leads to a ratio $\frac{\mu_\psi \{ \|\pi^{(T)} - \mu_\psi\| < \varepsilon \}}{\mu_{\psi'} \{ \|\pi^{(T)} - \mu_{\psi'}\| < \varepsilon \}}$ of order $\exp -T\eta$. Consequently, for $T \sim 10^8$ a divergence of order $\eta = 10^{-7}$ leads to a ratio of order $\exp(-10)$. Illustrations of this are given in section 4.

2.4.6 Other statistics related to Gibbs distributions.

The K-L divergence minimization can be completed with other standard criteria for which some analytical results are available in the realm of Gibbs distributions and thermodynamic formalism. Fluctuations of monomial averages about their mean are Gaussian, since Gibbs distribution obey a central limit theorem with a variance controlled by the second derivative of $P(\lambda)$. Then, using a χ^2 test seems natural. Examples are given in section 4. In order to compare the goodness-of-fit (GOF) for probability distributions of spike blocks, we propose at the descriptive level the box plots tests. On the other hand, quantitative methods to establish GOF are numerous and can be classified in families of 'test Statistics', the most important being the Power-Divergence methods (eg. Pearson- χ^2 test), the Generalized Kolmogorov-Smirnov (KS) tests (eg. the KS and the Watson-Darling test) and the Phi-Divergence methods (eg. Cramer-von Mises test)[20, 17]. Finally, to discriminate 2 Gibbs measures one can use the Neyman-Pearson criteria since large deviations results for the Neyman-Pearson risk are available in this case [50]. In the present paper we have limited our analysis to the most standard tests (diagonal representations, box plots, χ^2).

3 Application: parametric statistic estimation.

Let us now discuss how the previous piece of theory allows us to estimate, at a very general level, parametric statistics of spike trains.

We observe N neurons during a stationary period of observation T , assuming that statistics is characterized by an unknown Gibbs potential of range R . The algorithmic²⁰ procedure proposed here decomposes in three steps:

1. *Choosing a statistical model*, i.e. fixing the potential (6) (equivalently, the relevant monomials or "observables").
2. *Computing the empirical average of observables*, i.e. determine them from the raster, using eq. (24).
3. *Performing the parametric estimation*, i.e. use a variational approach to determine the Gibbs potential.

Let us describe and discuss these three steps, and then discuss the design choices.

²⁰The code is available at <http://enas.gforge.inria.fr/classGibbsPotential.html>

3.1 Choosing a model: rate, coincidence, spiking pattern and more.

3.1.1 The meaning of monomials.

In order to understand the power of representation of the proposed formalism, let us start reviewing a few elements discussed at a more theoretical level in the previous section.

We start with a potential limited to a unique monomial.

- If $\psi = \omega_i(0)$, its related average value measures the firing probability or *firing rate* of neuron i ;
- If $\psi(\omega) = \omega_i(0) \omega_j(0)$, we now measure the probability of spikes coincidence for neuron j and i , as pointed out at the biological level by, e.g. [28] and developed by [66];
- If $\psi(\omega) = \omega_i(\tau) \omega_j(0)$, we measure the probability of the event “neuron j fires and neuron i fires τ time step later” (or sooner according to the sign of τ); in this case the average value provides²¹ the *cross-correlation* for a delay τ and the auto-correlation for $i = j$;
- A step further, if, say, $\psi(\omega) = \omega_i(0) \omega_j(0) \omega_j(1)$, we now take into account triplets of spikes in a specific pattern (i.e. one spike from neuron i coinciding with two successive spikes from neuron j);

These examples illustrate the notion of “design choice”: the first step of the method being to choose the “question to ask”, i.e. what is to be observed over the data. In this framework, this translates in: “choosing the form of the potential”. Let us enumerate a few important examples.

3.1.2 Taking only rate or synchronization into account: Bernoulli and Ising potentials.

Rate potential are range-1 potentials, as defined before. Such models are not very interesting as such, but have two applications: they are used to calibrate and study some numerical properties of the present methods, and they are also used to compare the obtained conditional entropy with more sophisticated models.

Ising potentials have been introduced by Schneidman and collaborators in [67], taking rate and synchronization of neurons pairs, as studied in, e.g. [28]. This form is justified by the authors using the Jaynes argument.

Let us now consider potentials not yet studied, up to our best knowledge, in the present literature.

3.1.3 Taking rate and correlations into account: RPTD- k potentials.

This is a key example for the present study. On one hand, the present algorithmic was developed to take not only Bernoulli or Ising-like potential into account, but a

²¹Substracting the firing rates of i and j .

large class of statistical model, including a *general second order model* (redundant monomial being eliminated), i.e. taking rate, *auto-correlation* (parametrized by $\lambda_{i\tau}$) and *cross-correlation* (parametrized by $\lambda_{ij\tau}$) into account.

Being able to consider such type of model is an important challenge, because it provides a tool to analyze not only synchronization between neurons, but more general temporal relations (see e.g. [23, 28, 6] for important applications).

Let us now turn to a specific example related to the neuronal network dynamic analysis.

3.1.4 Taking plasticity into account: “STDP” potentials

In [12] we considered Integrate-and-Fire neural networks with Spike-Time Dependent Plasticity of type:

$$W'_{ij} = \varepsilon \left[r_d W_{ij} + \frac{1}{T} \sum_{t=-T_s}^{T+T_s} \omega_j(t) \sum_{u=-T_s}^{T_s} f(u) \omega_i(t+u) \right], \quad (34)$$

where W_{ij} is the synaptic weight from neuron j to neuron i , $-1 < r_d < 0$ a term corresponding to passive LTD, T a large time, corresponding to averaging spike activity for the synaptic weights update, and,

$$f(x) = \begin{cases} A_- e^{-\frac{x}{\tau_-}}, & x < 0, \quad A_- < 0; \\ A_+ e^{-\frac{x}{\tau_+}}, & x > 0, \quad A_+ > 0; \\ 0, & x = 0; \end{cases}$$

with $A_- < 0$ and $A_+ > 0$, is the STDP function as derived by Bi and Poo [4]. The shape of f has been obtained from statistical extrapolations of experimental data. $T_s \stackrel{\text{def}}{=} 2 \max(\tau_+, \tau_-)$ is a characteristic time scale. We argued that this synaptic weight adaptation rule produces, when it has converged, spike trains distributed according to a Gibbs distribution with potential:

$$\psi(\omega) = \sum_{i=0}^N \lambda_i^{(1)} \omega_i(0) + \sum_{i=0}^{N-1} \sum_{j=0}^{N-1} \lambda_{ij}^{(2)} \sum_{u=-T_s}^{T_s} f(u) \omega_i(0) \omega_j(u). \quad (35)$$

When considering a large number of neurons, it becomes difficult to compute and check numerically this joint probability over the whole population. Here, we propose to consider a subset \mathcal{P}_s of $N_s < N$ neurons. In this case, the effects of the rest of the population can be written as a bulk term modulating the individual firing rates and correlations of the observed population, leading to a marginal potential of the form:

$$\psi_{\mathcal{P}_s}(\omega) = \sum_{i \in \mathcal{P}_s} \lambda_i^{(1)'} \omega_i(0) + \sum_{i, j \in \mathcal{P}_s, 0}^{N-1} \sum_{j=0}^{N-1} \lambda_{ij}^{(2)'} \sum_{u=-T_s}^{T_s} f(u) \omega_i(0) \omega_j(u). \quad (36)$$

Here, the potential is a function of both past and future. A simple way to embed this potential in our framework, is to shift the time by an amount of T_s , using the stationarity assumption.

3.1.5 The general case: Typical number of observed neurons and statistics range.

The previous piece of theory allows us to take any statistics of range R , among any set of N neurons into account. At the numerical level, the situation is not that simple, since it appears, as detailed in the two next sections, that both the memory storage and computation load are in $O(2^{NR})$, except if the grammar is very restrictive, and the possible spike pattern blocks very sparse. Hopefully, we are going to see that estimation algorithms are rather efficient, thus do not lead to a complexity larger than $O(2^{NR})$.

It is clear that the present limitation is *intrinsic* to the problem, since we have *at least*, for a statistics of range R , to count the number of occurrences of blocks of N neurons of size R , and there are (at most) 2^{NR} of them. Fastest implementations must be based on the *partial* observation of only a subset of, e.g., the most preeminent occurrences.

Quantitatively, we consider “small” values of N and R , typically a number of neurons equal to $N \in \{1, \simeq 8\}$, and Markov chain of range $R = \{1, \simeq 16\}$, in order to manipulate quantities of dimension $N \leq 8$, and $R \leq 16$, and such that $N(R+1) \leq 18$.

3.2 Computing the empirical measure: prefix-tree construction.

For one sample ($\mathcal{N} = 1$), the empirical probability (25) of the block $[\omega]_{-D}^t$, $-D < t \leq 0$ is given by

$$\pi^{(T)}([\omega]_{-D}^t) = \frac{\#[\omega]_{-D}^t}{T}.$$

thus obtained counting the number of occurrence $\#[\omega]_{-D}^t$, $-D < t \leq 0$ of the block $[\omega]_{-D}^t$ in the sequence $[\omega]_{-T}^0$. Since we assume that dynamics is stationary we have, $\pi^{(T)}([\omega]_{-D}^t) = \pi^{(T)}([\omega]_0^{t+D})$.

We observe that the data structure size has to be of order $O(2^{NR})$ (lower if the distribution is sparse), but does not depends on T . Since many distributions are sparse (not all blocks occur, because the distribution is constrained by a grammar), it is important to use a sparse data structure, without storing explicitly blocks of occurrence zero.

Furthermore, we have to study the distribution at several ranges R and it is important to be able to factorize these operations. This means counting in one pass, and in a unique data structure, block occurrences of different ranges.

The chosen data structure is a tree of depth $R+1$ and degree 2^N . The nodes at depth D count the number of occurrences of each block $[\omega]_{-D+i}^t$, of length up to $D \leq R+1$ ²². It is known (see, e.g., [29] for a formal introduction) that this is a suitable data structure (faster to construct and to scan than hash-tables, for instance) in this context. It allows to maintain a computation time of order $O(TR)$, which does not depends on the structure size.

3.2.1 The prefix-tree algorithm.

Since we use such structure in a rather non-standard way compared to other authors, e.g. [29, 26], we detail the method here.

²²The code is available at <http://enas.gforge.inria.fr/classSuffixTree.html>.

We consider a spike train ω_{-T}^0 , where time is negative. The prefix-tree data structure for the present estimation procedure is constructed iteratively.

1. Each spiking pattern at time t , $\omega(t)$, is encoded by an integer $w(t)$.
2. This given, before any symbol has been received, we start with the empty tree consisting only of the root.
3. Then suppose for $-D < t \leq 0$ that the tree $\mathcal{T}([\omega]_{-T}^{t-1})$ represents $[\omega]_{-T}^{t-1}$. One obtains the tree $\mathcal{T}([\omega]_{-T}^t)$ as follows:
 - (a) One starts from the root and takes branches corresponding to the observed symbols $\omega(t-D+1), \dots, \omega(t)$.
 - (b) If one reaches a leaf before termination, one replaces this leaf by an internal node and extends on the tree.
 - (c) Each node or leaf has a counter incremented at each access, thus counting the number of occurrence $\#[\omega]_{-D}^t, -D < t \leq 0$ of the block $[\omega]_{-D}^t$ in the sequence $[\omega]_{-T}^0$.

The present data structure not only allows us to perform the empirical measure estimation over a period of time T , but can also obviously be used to aggregate several experimental periods of observation. It is sufficient to add all observations to the same data structure.

3.2.2 Generalization to a sliding window.

Though we restrict ourselves to stationary statistics in the present work, it is clear that the present mechanism can be easily generalized to the analysis of non-stationary data set, using a sliding window considering the empirical measure in $[t, t+T[$, then $[t+1, t+1+T[$, etc.. This is implemented in the present data structure by simply counting the block occurrences observed at time t and adding the block occurrences observed at time T , yielding a minimal computation load. The available implementation has already this functionality (see section 4.3.5 for an example).

3.3 Performing the parametric estimation

In a nutshell, the parametric estimation reduces to minimizing (27), by calculating the topological pressure $P(\psi) \equiv P(\lambda)$ using (14) and the related theorem. The process decomposes into the following steps.

3.3.1 Potential eigen-elements calculation.

It has been shown in the theoretical section that the Ruelle-Perron-Frobenius operator eigen-elements allows one to derive all characteristics of the probability distribution. Let us now describe at the algorithmic level how to perform these derivations.

1. The first step is to calculate the right-eigenvector $\mathbf{b}(\psi)$ of the $L(\psi)$ operator, associated to the highest eigenvalue, using a standard power-method series:

$$\begin{aligned} s^{(n)} &= \|L(\psi) \mathbf{v}^{(n-1)}\| \\ \mathbf{v}^{(n)} &= \frac{1}{s^{(n)}} L(\psi) \mathbf{v}^{(n-1)} \end{aligned}$$

where $\mathbf{v}^{(n)}$ is the n -th iterate of an initial vector $\mathbf{v}^{(0)}$ and $s^{(n)}$ is the n -th iterate of an initial real value $s^{(0)}$. With this method the pair $(s^{(n)}, \mathbf{v}^{(n)})$ converges to $(s(\psi), \mathbf{b}(\psi))$ as soon as $\mathbf{v}^{(0)}$ is not orthogonal to $\mathbf{b}(\psi)$. In our case, after some numerical tests, it appeared a good choice to either set $\mathbf{v}^{(0)}$ to an uniform value, or to use the previous estimated value of $\mathbf{b}(\psi)$, if available. This last choice is going to speed up the subsequent steps of the estimation algorithm.

The key point, in this iterative calculation, is that $L(\psi)$ is (hopefully) a sparse $2^{NR} \times 2^{NR}$ matrix, as outlined in the section 2.3.1. As a consequence calculating $L(\psi) \mathbf{v}$ is a $O(2^{N+NR}) \ll O(2^{2NR})$ operation, making explicit the grammar in the implementation.

The required precision on $(s(\psi), \mathbf{b}(\psi))$ must be very high, for the subsequent steps to be valid, even if the eigenvector dimension is huge (it is equal to 2^{NR}), therefore the iteration must be run down to the smallest reasonable precision level (10^{-24} in the present implementation).

We have experimented that between 10 to 200 iterations are required for an initial uniform step in order to attain the required precision (for $NR \in 2..20$), while less than 10 iterations are sufficient when starting with a previously estimated value.

From this 1st step we immediately calculate:

- (a) The topological pressure $P(\psi) = \log(s(\psi))$.
- (b) The normalized potential Ψ_w (this normalized potential is also stored in a look-up table). This gives us the transition matrix, which can be used to generate spike trains distributed according the Gibbs distribution μ_ψ and used as benchmarks in the section 4.

2. The second step is to calculate the left eigenvector $\langle \mathbf{b}(\psi)$, this calculation having exactly the same characteristics as for $\mathbf{b}(\psi)$.

From this 2nd step one immediately calculates:

- (a) The Gibbs probability of a block w given by (15), from which probabilities of any block can be computed (section 2.3.7).
- (b) The theoretical value of the observables average $\mu_\psi(\phi_l)$, as given in (16).
- (c) The theoretical value of the distribution entropy $h[\mu_\psi]$, as given in (18).

After both steps, we obtain all useful quantities regarding the related Gibbs distribution: probability measure, observable value prediction, entropy. These algorithmic loops are direct applications of the previous piece of theory and show the profound interest of the proposed framework: given a Gibbs potential, all other elements can be derived directly.

3.3.2 Estimating the potential parameters.

The final step of the estimation procedure is to find the parameters λ such that the Gibbs measure fits at best with the empirical measure. We have discussed why minimizing (27) is the best choice in this context. Since $h(\pi^{(T)})$ is a constant with respect to λ , it is equivalent to minimize $\tilde{h}[\psi_\lambda]$ eq. (29), where $\mu_\psi(\phi_l)$ is given by (16). Equivalently, we are looking for a Gibbs distribution μ_ψ such that $\frac{\partial P[\psi_\lambda]}{\partial \lambda_l} = \pi^{(T)}(\phi_l)$ which expresses that $\pi^{(T)}$ is tangent to P at ψ_λ [38].

3.3.3 Matching theoretical and empirical observable values.

As pointed out in the theoretical part, the goal of the estimation is indeed to find the parameters λ for which theoretical and empirical observable values match. The important point is that this is exactly what is performed by the proposed method: minimizing the criterion until a minimum is reached, i.e. until the gradient vanishes corresponding to a point where $\mu_\psi(\phi_l) = \pi^{(T)}(\phi_l)$, thus where theoretical and empirical observable values are equal. Furthermore, this variational approach provides an effective method to numerically obtain the expected result.

At the implementation level, the quantities $\pi^{(T)}(\phi_l)$ are the empirical averages of the observables, i.e. the observable averages computed on the prefix tree. They are computed once from the prefix tree. For a given λ , $P(\lambda)$ is given by step 1.a of the previous calculation, while $\mu_\psi(\phi_l)$ is given by the step 2.b. It is thus now straightforward²³ to delegate the minimization of this criterion to any standard powerful non-linear minimization routine.

We have implemented such a mechanism using the GSL²⁴ implementation of non-linear minimization methods. We have also made available the GSL implementation of the simplex algorithm of Nelder and Mead which does not require the explicit computation of a gradient like in eq. (29). This alternative is usually less efficient than the previous methods, except in situations, discussed in the next section, where we are at the limit of the numerical stability. In such a case the simplex method is still working, whereas other methods fail.

²³Considering a simple gradient scheme, there is always a $\varepsilon^k > 0$, small enough for the series λ_l^k and \tilde{h}^k , defined by:

$$\lambda_l^{k+1} = \lambda_l^k + \varepsilon^k \frac{\partial \tilde{h}}{\partial \lambda_l}(\lambda_l^k)$$

$$0 \leq \tilde{h}^{k+1} < \tilde{h}^k,$$

to converge, as a bounded decreasing series, since:

$$\tilde{h}^{k+1} = \tilde{h}^k - \varepsilon^k \left| \frac{\partial \tilde{h}}{\partial \lambda_l} \right|^2 + O((\varepsilon^k)^2).$$

²⁴The GSL <http://www.gnu.org/software/gsl> multi-dimensional minimization algorithms taking the criteria derivatives into account used here is the Fletcher-Reeves conjugate gradient algorithm, while other methods such as the Polak-Ribiere conjugate gradient algorithm, and the Broyden-Fletcher-Goldfarb-Shannon quasi-Newton method appeared to be less efficient (in precision and computation times) on the benchmarks proposed in the result section. Anyway, the available code <http://enas.gforge.inria.fr/classIterativeSolver.html> allows us to consider these three alternatives, thus allowing to tune the algorithm to different data sets.

3.3.4 Measuring the precision of the estimation.

Once the quantity $\tilde{h}[\psi] = P[\psi] - \pi^{(T)}(\psi)$ (eq. (29)) has been minimized the Kullback-Leibler divergence $d(\pi^{(T)}, \mu_\psi) = \tilde{h}[\psi] - h(\pi^{(T)})$ determines a notion of “distance” between the empirical measure $\pi^{(T)}$ and the statistical model μ_ψ . Though it is not necessary to compute $d(\pi^{(T)}, \mu_\psi)$ for the comparison of two statistical models $\mu_\psi, \mu_{\psi'}$, the knowledge of $d(\pi^{(T)}, \mu_\psi)$, even approximate, is a precious indication of the method precision. This however requires the computation of $h(\pi^{(T)})$.

Though the numerical estimation of $h(\pi^{(T)})$ is a far from obvious subject, we have implemented the entropy estimation using definitions (3) and (4). In order to interpolate the limit (4), we have adapted an interpolation method from [29] and used the following interpolation formula. Denote by $h(\pi^{(T)})^{(n)}$ the entropy estimated from a raster plot of length T , considering cylinders of size n . We use the interpolation formula $h(\pi^{(T)})^{(n)} \simeq h^\infty + \frac{k}{n^c}$, where $h^\infty, k, c > 0$ are free parameters, with $h(\pi^{(T)})^{(n)} \rightarrow h^\infty$, as $n \rightarrow +\infty$. The interpolation formula has been estimated in the least square sense, calculating $h(\pi^{(T)})^{(n)}$ on the prefix-tree. The formula is linear with respect to h^∞ and k , thus has a closed-form solution with respect to these two variables. Since the formula is non-linear with respect to c , an iterative estimation mechanism is implemented.

3.4 Design choices: genesis of the algorithm.

Let us now discuss in details the design choices behind the proposed algorithm.

The fact that we have an implementation able to efficiently deal with higher-order dynamics is the result of computational choices and validations, important to report here, in order for subsequent contributor to have the benefit of this part of the work.

3.4.1 Main properties of the algorithm.

Convexity. As indicated in the section 2.4.4 there is a unique minimum of the criterion. However, if $\psi^{(est)}$ contains monomials which are not in ψ , the procedure converges but there is an indeterminacy in the λ_i 's corresponding to exogenous monomials. The solution is not unique, there is a subspace of equivalent solutions. The rank of the topological pressure Hessian is an indicator of such a degenerate case. Note that these different situations are not inherent to our procedure, but to the principle of finding an hidden probability by maximizing the statistical entropy under constraints, when the full set of constraints is not known [21].

Finite sample effects. As indicated in the section 2.4.5 the estimations crucially depend on T . This is a central problem, not inherent to our approach but to all statistical methods where one tries to extract statistical properties from finite empirical sample. Since T can be small in practical experiments, this problem can be circumvented by using an average over several samples. In the present thermodynamic formalism it is possible to have an estimation of the size of fluctuations as a function of the potential, using the central limit theorem and the fact that the variance of fluctuations is given by the second derivative of the topological pressure. This is a further statistical test

where the empirical variance can be easily measured and compared to the theoretical predictions.

Numerical stability of the method. Two factors limitate the stability of the method, from a numerical point of view.

The first factor is that the RPF operator is a function of the *exponential* of the potential $\psi = \sum_l \lambda_l \phi_l$. As a consequence, positive or negative values of ψ yield huge or vanishing value of L_ψ , and numerical instabilities easily occurs.

However, though numerical instabilities are unavoidable, the good news is that they are easily detected, because we have introduced a rather large set of numerical tests in the code:

1. Negligible values (typically lower than 10^{-4}) are set to zero, implicitly assuming that they correspond to hidden transition in the grammar.
2. Huge value (typically higher than 10^4) generate a warning in the code.
3. Several coherent tests regarding the calculation of the RPF eigen-elements are implemented: we test that the highest eigenvalue is positive (as expected from the RPF theorem), and that the left and right RPF related eigenvectors yield equal eigenvalues, as expected; we also detect that the power-method iterations converge in less than a maximal number of iteration (typically 2^{10}). We never found this spurious condition during our numerical tests. When computing the normalized potential (19), we verify that the right eigenvalue is 1 up to some precision, and check that the normal potential is numerically normalized (i.e. that the sum of probabilities is indeed 1, up to some “epsilon”).

In other words, we have been able to use all what the piece of theory developed in the previous section makes available, to verify that the numerical estimation is valid.

The second factor of numerical imprecision is the fact that some terms $\lambda_l \phi_l$ may be negligible with respect to others, so that the numerical estimation of the smaller terms becomes unstable with respect to the imprecision of the higher ones. This has been extensively experimented, as reported in the next section.

Relation with entropy estimation. The construction of a prefix-tree is also the basis of efficient entropy estimation methods [29, 68]. See [26] for a comparative about entropy estimation of one neuron spike train (binary time series). Authors numerically observed that the context-tree weighting methods [42] is seen to provide the most accurate results. This, because it partially avoids the fact that using small word-lengths fails to detect longer-range structure in the data, while with longer word-lengths the empirical distribution is severely under-sampled, leading to large biases. This statement is weakened by the fact that the method from [68] is not directly tested in [26], although a similar prefix-tree method has been investigated.

However the previous results are restrained to relative entropy estimation of “one neuron” whereas the analysis of entropy of a *group of neurons* is targeted if we want to better investigate the neural code. In this case [68] is directly generalizable to non-binary (thus multi-neurons) spike trains, whereas the context-tree methods seems in-

trinsically limited to binary spike-trains [42], and the numerical efficiency of these methods is still to be studied at this level.

Here, we can propose an estimation for the KS-entropy from eq. (18). Clearly, we compute here the entropy of a Gibbs statistical model μ_ψ while methods above try to compute this entropy from the raster plot. Thus, we do not solve this delicate problem, but instead, propose a method to benchmark these methods from raster plots obeying a Gibbs statistics, where the Gibbs distribution approaches at best the empirical measures obtained from experiments.

3.4.2 Key aspects of the numerical implementation.

Estimating the grammar from the empirical measure.

The grammar defined in (13) is implemented as a Boolean vector indexed by w and estimated by observing, in a prefix-tree of depth at least $R + 1$, whose blocks $[\omega]_{-R-1}^0$ occur at least once (allowed transition). We make therefore here the (unavoidable) approximation that unobserved blocks correspond to forbidden words (actually, our implementation allows to consider that a block is forbidden if it does not appear more than a certain threshold value). There is however, unless a priori information about the distribution is available, no better choice. The present implementation allows us to take into account such a priori information, for instance related to global time constraints on the network dynamics, such as the refractory period. See [12] for an extended discussion.

Potential values tabulation.

Since the implementation is anyway costly in terms of memory size, we have chosen to pay this cost but obtaining the maximal benefit of it and we used as much as possible tabulation mechanisms (look-up tables) in order to minimize the calculation load. All tabulations are based on the following binary matrix:

$$\mathbf{Q} \in \{0, 1\}^{L \times 2^{NR}},$$

with $\mathbf{Q}_{l,w} = \phi_l([\omega]_{-R}^0)$, where w is given by (10). \mathbf{Q} is the matrix of all monomial values, entirely defined by the choice of the parameter dimensions N , R and D . It corresponds to a “look-up table” of each monomial values where w encodes $[\omega]_{-R}^0$. Thus the potential (6) writes $\psi_w = (\mathbf{Q}\lambda)_w$. We thus store the potential exponential values as a vector and get values using a look-up table mechanism, speeding-up all subsequent computations.

This allows to minimize the number of operations in the potential eigen-elements calculation.

3.4.3 Appendix: About other estimation alternatives.

Though what is proposed here corresponds, up to our best knowledge, to the best we can do to estimate a Gibbs parametric distribution in the present context, this is obviously not the only way to do it, and we have rejected a few other alternatives, which

appeared less suitable. For the completeness of the presentation, it is important to briefly discuss these issues.

Avoiding RPF right eigen-element's calculation. In the previous estimation, at each step, we have to calculate step 1 of the RPF eigen-element's derivation for the criterion value calculation and step 2 of the RPF eigen-element's derivation for the criterion gradient calculation. These are a costly $O(2^{N+NR})$ operations.

One idea is to avoid step 2 and compute the criterion gradient numerically. We have explored this track: we have calculated $\frac{\partial \tilde{h}}{\partial \lambda_l} \simeq \frac{\tilde{h}(\lambda_l + \varepsilon) - \tilde{h}(\lambda_l - \varepsilon)}{2\varepsilon}$ for several order of magnitude, but always found a poorer convergence (more iteration and a biased result) compared to using the closed-form formula. In fact, each iteration is not faster, since we have to calculate \tilde{h} at two points thus, to apply step 1, at least two times. This variant is thus to be rejected.

Another idea is to use a minimization method which does not require the calculation of the gradient: we have experimented this alternative using the simplex minimization method, instead of the conjugate gradient method, and have observed that both methods correctly converge towards a precise solution in most cases, while the conjugate gradient method is faster. However, there are some cases with large range potential, or at the limit of the numerical stability where the simplex method may still converge, while the other does not.

Using a simple Gibbs form. Using the Gibbs form

$$\mu_\Psi [w_t, \dots, w_{t+n}] = \frac{e^{\sum_{k=t}^{t+n} \Psi_{w_k}}}{Z_n}, \text{ with } Z_n = \sum_{w_t, \dots, w_{t+n}} e^{\sum_{k=t}^{t+n} \Psi_{w_k}},$$

where Z_n is a constant, could provide an approximation of the right Gibbs distribution and of the topological pressure, avoiding the power-method internal loop. Furthermore, instead of a costly $O(2^{N+NR})$ operation, calculating Z_n (and derivatives) would require a simple scan of the prefix-tree (since values are calculated at each step weighted by the empirical measure values) thus $O(2^{NR})$ operations. This apparent gain is unfortunately impaired since the amount of calculation is in fact rather heavy. Moreover, as widely commented on section 2, the result is biased with a *non negligible* additional bias increasing with the range R of the potential. Finally, it has been observed as being slower than for the basic method.

About analytical estimation of the RPF eigen-element's. The costly part of the RPF eigen-element's computation is the estimation of the highest eigenvalue. It is well-known that if the size of the potential is lower than five, there are closed-form solutions, because this problem corresponds to finding the root of the operator characteristic polynomial. In fact, we are going to use this nice fact to cross-validate our method in the next section. However, except for toy's potentials (with $2^{NR} < 5 \Leftrightarrow NR \leq 2$!), there is no chance that we can not do better than *numerically* calculating the highest eigenvalue.

And the power method is known as the most powerful way to do it, in the general case. We thus have likely optimal choices at this stage.

Using other approximations of the KL-divergence criterion. Let us now discuss another class of variants: the proposed KL-divergence criterion in (22) and its empirical instantiation in (27) are not the only one numerical criterion that can be proposed in order to estimate the Gibbs distribution parameters. For instance, we have numerically explored approximation of the KL-divergence of the form:

$$d(v, \mu) \simeq \sum_{n=R}^{R'} \frac{\alpha_n}{n} \sum_{[\omega]_0^{n-1}} v([\omega]_0^{n-1}) \log \left[\frac{v([\omega]_0^{n-1})}{\mu([\omega]_0^{n-1})} \right],$$

and have obtained coherent results (for $\alpha_n = 1$), but not quantitatively better than what is observed by the basic estimation method, at least for the set of performed numerical tests.

All these variants correspond to taking into account the same kind of criterion, but some other weighted evaluations of the empirical average of the observable. There is no reason to use it unless some specific a priori information on the empirical distribution is available.

Another interesting track is to use (19) which allows us to write a KL-divergence criterion, not on the probability block, but on the conditional probability block, as proposed in [14, 15] in a different context. We have considered this option. However a straightforward derivation allows one to verify, that this in fact corresponds the same class of criterion but with a different empirical observable average estimation. At the numerical level, we did not observe any noticeable improvement.

Using score matching based estimation. We are here in a situation where we have to estimate a parametric statistical distribution, whose closed-form is given up to a scale factor Z_n . Such model contains a normalization constant whose computation may be considered as too difficult for practical purposes, as it is the case for some maximum likelihood estimations. Score-matching methods [32] are based on the gradient of the log-density with respect to the data vector, in which the normalization constant is eliminated. However, the estimation criterion is no more the KL-divergence, and there is no guaranty that the obtained solution is not biased with respect to a well-defined statistical quantity. As such it is another candidate to estimate Gibbs distribution. However, thanks to the eigen decomposition of the RPF operator, we do not need to use this trick, since we obtain a tractable calculation of the normalization constant at each step of the estimation and can minimize a well-defined criterion, as proposed in this paper.

We have numerically checked such modification of the criterion in which we do not consider the KL-divergence criterion, but the *ratio* between two conditional probabilities, as defined in (19). Considering this ratio allows to eliminate the scale factor Z_n . This is the same spirit as score matching based estimation, more precisely, it corresponds to a discrete form of it, where the gradient of the log-density is replaced by finite

difference. We have obtain correct results for simple forms of potential, but have experimented that the method is numerically less robust than using the unbiased method developed in this paper. This confirms that using the eigen-decomposition of the RPF operator, is the key for numerically stable estimations of such parametric statistics.

Estimation in the case of a normalized potential. In the case where the potential is normalized, the criterion (29) is a simple linear criterion, thus unbounded and its minimization is meaningless. In this singular case, its is obvious to propose another criterion for the estimation of the parameters. A simple choice is to simply propose that the theoretical likelihood of the measure matches the estimated one, in the *least square sense*. This has been integrated in the available code.

4 Results

4.1 Basic tests: validating the method

4.1.1 Method

Knowing the potential ψ , it is easy to generate a spike train of length T , distributed according to μ_ψ , using the Chapman-Kolmogorov equations (20). Thus, we have considered several examples of Gibbs potentials, where, starting from a sample raster plot $[\omega]_{-T}^0$ distributed according to μ_ψ , we use our algorithm to recover the right form of ψ .

Given a potential of range- R of the parametric form (6) and a number of neurons N we apply the following method:

1. Randomly choosing the parameter's values $\lambda_l, l = 1 \dots L$ of the Gibbs potential;
2. Generating a spike train realization of length T ;
3. From these values re-estimating a Gibbs potential:
 - (a) Counting the block occurrences, thus the probabilities $\pi^{(T)}$ from the prefix-tree,
 - (b) Minimizing (29), given $\pi^{(T)}$, as implemented by the proposed algorithm.
 - (c) Evaluating the precision of the estimation as discussed in the previous section.

In the previous method, there is a way to simulate “infinite” ($T = +\infty$) sequences, by skipping step 2., and filling the prefix-tree in step 3.a directly by the exact probability $\mu_\psi(w)$ of the blocks w .

At a first glance, this loop seems to be a “tautology” since we re-estimate the Gibbs potential parameters from a one-to-one numerical process. However, this is not the case for three reasons:

1. For $T = +\infty$ using the same potential for the prefix-tree generation and for the parameters estimation, must yield the same result, but *up to the computer numerical precision*. This has to be controlled due to the non-linear minimization loop in huge dimension. This is obviously also a way to check that the code has no mistake.
2. For $T < +\infty$ using the same potential allows us to study the numerical precision of the estimation in the realistic situation of finite size data set, providing quantitative estimations about the truncation effects to be expected.
3. Using different potentials between simulated data generation and the parameters value estimation allows us to study numerically to which extends we can only correctly estimate the parameter's values, even if huge state vectors are involved. Quantitative errors are obtained. We can also perform comparison between different statistical models, as detailed in the sequel.

4.1.2 An illustrative example to understand what the algorithm calculates

Let us start with very simple example, for which we can make explicit what the algorithm calculates, thus helping the reader to understand in details what the output is.

We consider a situation where the number L of parameters λ_l is known (only the values of the λ_l 's are unknown). We start from rather basic examples and then increase their complexity. In the first examples analytical expression for the topological pressure, entropy, RPF eigen-vectors and invariant measure are available. Thus we can check that we re-obtain, from the estimation method, the related values up to the numerical imprecision.

One neuron and range-2. Here $\psi(\omega) = \lambda_1 \omega_0(0) + \lambda_2 \omega_0(0) \omega_0(1)$. We obtain analytically:

$$\begin{aligned}
s(\psi) &= \frac{1+B+\sqrt{(1-B)^2+4A}}{2}, \\
P(\psi) &= \log s(\psi), \\
\langle \mathbf{b}(\psi) \rangle &= (1, s(\psi) - 1, A, B(s(\psi) - 1),) \\
\mathbf{b}(\psi) \rangle &= (s(\psi) - B, s(\psi) - B, 1, 1)^T, \\
\mu_\psi &= \frac{1}{s(\psi)^2+A-B} (s(\psi) - B, A, A, B(s(\psi) - 1)), \\
h[\mu_\psi] &= \log(s(\psi)) - \lambda_1 \frac{\partial s(\psi)}{\partial \lambda_1} - \lambda_2 \frac{\partial s(\psi)}{\partial \lambda_2} \\
r &= \frac{A+B(s(\psi)-1)}{s(\psi)^2+A-B}, \\
C &= \frac{B(s(\psi)-1)}{s(\psi)^2+A-B},
\end{aligned}$$

with $A = e^{\lambda_1} = e^{\psi_{10}}$, $B = e^{\lambda_1+\lambda_2} = e^{\psi_{11}}$ and where T denotes the transpose. We remind that the index vector encodes spike blocs by eq. (10). Thus, the first index (0) corresponds to the bloc 00, 1 to 01, 2 to 10 and 3 to 11. r is the firing rate, C the probability that the neuron fires two successive time steps. This is one among the few models for which a closed-form solution is available.

The following numerical verifications have been conducted. A simulated prefix-tree whose nodes and values has been generated using (6) with $\lambda_1 = \log(2), \lambda_2 = \log(2)/2$. We have run the estimation program of λ_i 's and have obtained the right values with a precision better than 10^{-6} . We also obtain a precision better than 10^{-6} for $s(\psi), r, C, h[\mu_\psi]$. This first test simply states that the code has no mistake.

A step further, we have used this simple potential to investigate to which extends we can detect if the model is of range-1 (i.e. with $\lambda_2 = 0$) or range-2 (i.e. with a non-negligible value of λ_2). To this purpose, we have generated a range-2 potential and have performed its estimation using a range-1 and a range-2 potential, comparing the entropy difference (Fig. 4.1.2).

As expected the difference is zero for a range-2 model when $\lambda_2 = 0$, and this difference increases with λ_2 . Less obvious is the fact that curves saturate for high values of λ_2 . Indeed, because of the exponential function, high values of λ yield huge or vanishing values of the RPF operator, thus numerical instabilities. This instability is detected by our algorithm. Note that values of λ larger than 10 in absolute value have little sense from a statistical analysis of spike trains perspective.

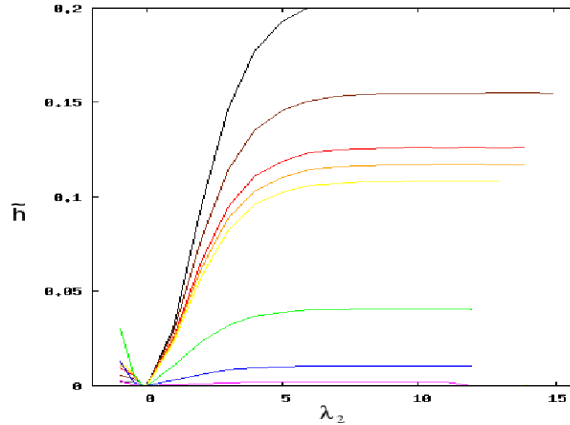


Figure 1: Entropy difference, using \tilde{h} , defined in (29), between the estimations of a range-1 and a range-2 model. The range-2 model writes $\phi = -\lambda_1 \omega_0(0) - \lambda_2 \omega_0(0) \omega_0(1)$ for $\lambda_1 = \{-1$ (black), -0.5 (brown), -0.2 (red), -0.1 (orange), 0 (green), 1 (blue), 2 (Magenta) $\}$. λ_2 is a free parameter, in abscissa of this curve. The range-1 corresponds to $\lambda_2 = 0$.

We also have generated a range-1 potential and have performed its estimation, using a range-1 versus a range-2 model, and found always that using range-2 model is as good as using a model of range-1 (not shown).

Two neurons and range-2 (Ising). Here $\psi(\omega) = \lambda_1 \omega_1(0) + \lambda_2 \omega_2(0) + \lambda_3 \omega_1(0) \omega_2(0)$. The largest eigenvalue of the RPF operator is $Z = s(\psi) = A + B + C + D$, with $A = 1, B = e^{\lambda_1}, C = e^{\lambda_2}, D = e^{\lambda_1 + \lambda_2 + \lambda_3}$ and the topological pressure is $\log s(\psi)$. Here the Gibbs distribution has the classical form. We still obtain numerical precision better than 10^{-4} , for standard values of λ , e.g., $\lambda_1 = 1, \lambda_2 = \log(2), \lambda_3 = \log(2)/2$.

Two neurons and pattern of spikes. A step further, we have considered $\psi(\omega) = \lambda_1 \omega_1(0) + \lambda_2 \omega_2(0) + \lambda_3 \omega_1(0) \omega_2(1) \omega_1(2)$, and $\psi(\omega) = \lambda_1 \omega_1(0) + \lambda_2 \omega_2(0) + \lambda_3 \omega_1(0) \omega_2(1) \omega_2(2) \omega_3(3)$, for random values drawn in $] -1, 0[$, i.e., considering the statistical identification of *spike patterns*. We still obtain numerical precision better than 10^{-3} , for these standard values of λ , though the precision decreases with the number of degrees of freedom, as expected, while it increases with the observation time. This is investigated in details in the remainder of this section.

When considering larger neuron N and range- R the main obstacle toward analytical results is the Galois theorem which prevent a general method for the determination of the largest eigenvalue of the RPF operator. Therefore, we only provide numerical results obtained for more general potentials.

4.1.3 Gibbs potential precision paradigm: several neurons and various ranges.

In order to evaluate the numerical precision of the method, we have run the previous benchmark considering potentials with all monomial of degree less or equal to 1, and less or equal to 2, at a various ranges, with various numbers of neurons. Here we have chosen $T = +\infty$ and used the same potential for the prefix-tree generation and for the parameters value estimation. The computation time is reported in Table 1 and the numerical precision in Table 2, for $NR \leq 16$. This benchmark allows us to verify that there is no “surprise” at the implementation level: computation time increases in a supra-linear way with the potential size, but, thanks to the chosen estimation method, remains tractable in the size range compatible with available memory size. This is the best we can expect, considering the intrinsic numerical complexity of the method. Similarly, we observe that while the numerical precision decreases when considering large size potential, the method remains stable. Here tests has been conducted using the standard 64-bits arithmetic, while the present implementation can easily be recompiled using higher numerical resolution (e.g. “long double”) if required.

A step further, this benchmark has been used to explore the different variants of the estimation method discussed in the previous section (avoiding some RPF eigen-element’s calculation, using other approximations of the KL-divergence criterion, ..) and fix the details of the proposed method.

Table 1: Cpu-time order of magnitude in second (using Pentium M 750 1.86 GHz, 512Mo of memory), for the estimation of a potential with all monomial of degree less or equal to 1, for ψ_1 and less or equal to 2, for ψ_2 , (i.e., $\psi_1(\omega) = \sum_{i=0}^{N-1} \lambda_i \omega_i(0)$, $\psi_2(\omega) = \sum_{i=0}^{N-1} \lambda_i \omega_i(0) + \sum_{i=0}^{N-1} \sum_{j=0}^{i-1} \sum_{\tau=-T_s}^{T_s} \lambda_{ij\tau} \omega_i(0) \omega_j(\tau)$) at a range- $R = 2T_s + 1$ with N neurons. We clearly observe the exponential increase of the computation time. Note that the present implementation is not bounded by the computation time, but simply by the exponential increase of the memory size.

ψ_1	R=1	R=2	R=4	R=8	R=16	ψ_2	R=1	R=2	R=4	R=8	R=16
N=1	2.0e-06	3.0e-06	8.0e-06	7.8e-05	2.9e-01	N=1	4.5e-16	4.0e-06	4.0e-06	7.2e-04	3.7e-02
N=2	4.0e-06	1.0e-06	3.0e-05	6.7e-02		N=2	3.0e-06	5.0e-06	4.0e-04	1.1e+00	
N=4	1.3e-05	3.8e-05	8.3e-02			N=4	1.9e-05	1.2e-03	3.6e+00		
N=8	2.4e-03	3.2e-01				N=8	6.6e-03	6.2e-01			

Table 2: Numerical precision of the method using synthetic data, for the estimation of ψ_1 and ψ_2 , at a range- R with N neurons. The Euclidean distance $|\bar{\lambda} - \tilde{\lambda}|$ between the estimated parameter's value $\tilde{\lambda}$ and the true parameter's value $\bar{\lambda}$ is reported here, when the $\bar{\lambda}_i$'s are randomly drawn in $[-1, 1]$. We clearly observe the error increase, but the method remaining numerically stable.

ψ_1	R=1	R=2	R=4	R=8	R=16	ψ_2	R=1	R=2	R=4	R=8	R=16
N=1	5.0e-09	2.2e-02	6.3e-03	1.3e-02	6.9e-03	N=1	1.1e-10	1.9e-02	7.2e-03	4.8e-03	9.2e-02
N=2	1.1e-08	1.3e-02	9.2e-03	5.2e-03		N=2	1.1e-09	4.8e-03	3.7e-03	2.3e-03	
N=4	8.0e-09	8.5e-03	6.8e-03			N=4	3.7e-08	2.6e-03	5.8e-02		
N=8	3.8e-08	5.1e-03				N=8	6.0e-06	2.4e-02			

4.2 More general tests: applying the method

4.2.1 Test framework.

In order to test more general potentials for $N = 2$ neurons we explicit here the forms (7), (8), (9), where $k \in \mathbb{N}$:

$$\begin{aligned}
 \text{Ising : } \psi(\omega) &= \lambda_1 \omega_1(0) + \lambda_2 \omega_2(0) + \lambda_3 \omega_1(0) \omega_2(0). \\
 \text{RPTD} - k : \psi(\omega) &= \lambda_1 \omega_1(0) + \lambda_2 \omega_2(0) + \sum_{i=-k}^{i=k} \hat{\lambda}_i \omega_1(0) \omega_2(i). \\
 \text{PTD} - k : \psi(\omega) &= \sum_{i=-k}^{i=k} \hat{\lambda}_i \omega_1(0) \omega_2(i).
 \end{aligned} \tag{37}$$

test 1 (estimation precision). Given a selected potential of form (37) we choose randomly its coefficients $\bar{\lambda}_i$ from an uniform distribution on $[-2, 0]$ and we generate a spike-train of length $T = 4 \times 10^8$. Then we construct a prefix-tree from a sample of length $T_0 \ll T$ (typically $T_0 = 10^7$) taken from the generated spike-train. For each sample of length T_0 we propose a randomly chosen set of ‘‘initial guess’’ coefficients, used to start the estimation method, distributed according to $\tilde{\lambda}_i^{(0)} = \bar{\lambda}_i(1 + (U[0, 1] - 0.5)x/100)$, where x is the initial percentage of bias from the original set of generating coefficients and $U[0, 1]$ is a uniform random variable on $[0, 1]$. Call $\tilde{\lambda}_i$ the values

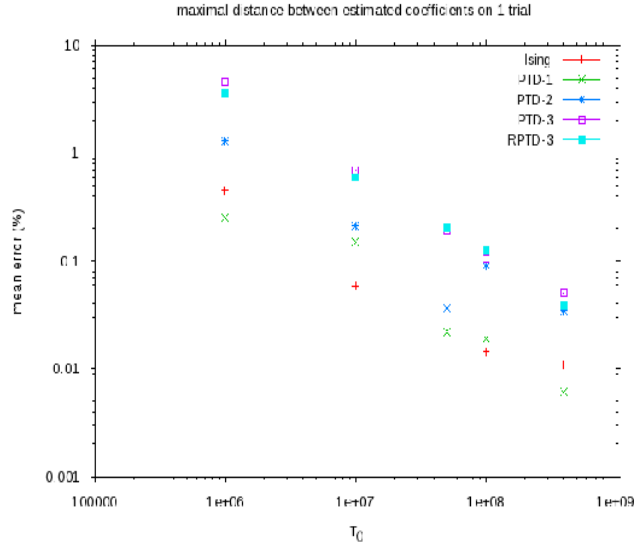


Figure 2: Mean error (in percentage) vs T_0 size.

obtained after convergence of the algorithm. Results show that:

- (i) the error $E(|\tilde{\lambda}_l - \bar{\lambda}_l|)$ increases with the range of the potential and it decreases with T_0 ;
- (ii) the error is independent of the initial bias percentage (see figs 4.2.1);
- (iii) $\tilde{h}[\psi] = P[\psi] - \pi^{(T)}(\psi)$ is fairly constant with respect to the length T_0 (not shown).

Test 2 (Models comparison). We select a potential form ψ from those proposed in (37); we choose randomly its coefficients $\bar{\lambda}_l$ from an uniform distribution in $[-2, 0]$; we generate a spike-train of length $T = 1 \cdot 10^8$ and we construct the prefix-tree with the spike-train obtained. Using this prefix-tree we estimate the coefficients $\lambda_i^{\psi_m}$ that minimizes the KL divergence for several statistical models ψ_m proposed in (37). The coefficients $\lambda_i^{\psi_m}$ and $\tilde{h} = P[\psi_m] - \pi^{(T)}(\psi_m)$ are averaged over 20 samples and error bars are computed. Results show that :

- (i) The 'best' statistical models (i.e the ones with lowest mean value KL divergence) have the same monomials as the statistical model that generated the spike-train, plus, possibly additional monomials. For example, in (37), **RPTD-1** contains **Ising**, and also the **PTD-1** but not **PTD-2**. We choose the model with the minimal number of coefficients in agreement with section 2.4.4.

- (ii) The value of the additional coefficients of an over-estimated model (corresponding to monomials absent in the corresponding potential) are almost null up to the numerical error.
- (iii) For all the 'best' suited statistical models (in the sense of (i)), the criterion $\tilde{h}[\psi]$ (29) averaged over trials, is fairly equal for these models up to a difference of order $\delta \approx 10^{-6}$, and the difference with respect to other types of statistical models is at least of 4 orders of magnitude lower. We recall that, according to section 2.4.5, the deviation probability is of order to $\exp(-\delta T)$. After estimation from a raster generated with an Ising model, the ratio of the deviation probabilities (33) between an **Ising** and a **RPTD-1** model is $\sim \eta = \exp(0.0000115 \times 10^8)$, while between the **Ising** and the **PTD-3** $\sim \eta = \exp(0.00072 \times 10^8)$ meaning that the **PTD-3** provide a worst estimation.
- (iv) The predicted probability of words corresponds very well with the empirical value.

In order to extend the model comparison we introduce the following notations: let w be a word (encoding a spiking pattern) of length R , $P_{est}(w)$ its mean probability over trials calculated with the estimated potential, $P_{emp}(w)$ its mean empirical average over trials (i.e average of form (24) including a time average $\pi^{(T)}$ and a sample average, where the samples are contiguous pieces of the raster of length $T_0 \ll T$), and $\sigma_{emp}(w)$ the standard deviation of $P_{emp}(w)$. We now describe the comparison methods.

We first use the box-plot method [25] which is intended to graphically depict groups of numerical data through their 'five-number summaries' namely: the smallest observation (sample minimum), lower quartile (Q1), median (Q2), upper quartile (Q3), and largest observation (sample maximum)²⁵. Figure 4.2.1 shows, in log-scale, the box-plot for the distribution of the quantity defined as:

$$\varepsilon(w) = |(P_{est}(w) - P_{emp}(w)) / \sigma_{emp}(w)| \quad (38)$$

that is taken as a weighted measure of the deviations. We have considered this distribution when it takes into account, either all the words up to a given size R_{max} , or only the words of that given size. There is no visual difference for $R_{max} = 7$. The results shows that only models containing the generating potential have the lower deviations value with very similar box. On the other hand a "bad" statistical model shows a much more extended error distribution .

Finally a χ^2 estimation is computed as $\chi^2 = \frac{1}{N_{words}-L} \sum_w \varepsilon(w)^2$ where $\varepsilon(w)$ is given by (38). Values are reported in tables 3, using all words or only those of size R_{max} . Since the number of words is high, it is clear that the lower the error, the lower the

²⁵ The largest (smallest) observation is obtained using parameter dependent bounds, or "fences", to filter aberrant uninteresting deviations. Call $\beta = Q3 - Q1$ and let k denote the parameter value, usually between 1.0 and 2.0. Then the bound correspond to $Q3 + k\beta$ for the largest observation (and for the smallest one to $Q1 - k\beta$). A point x found above (below) is called "mild-outlier" if $Q3 + k < x < Q3 + 2k\beta$ (respectively, $Q1 - 2k\beta < x < Q3 - k\beta$) or extreme outlier if $x > Q3 + 2k\beta$ (respectively, $x < Q1 - 2k\beta$). We have used a fence coefficient $k = 2.0$ to look for outliers.

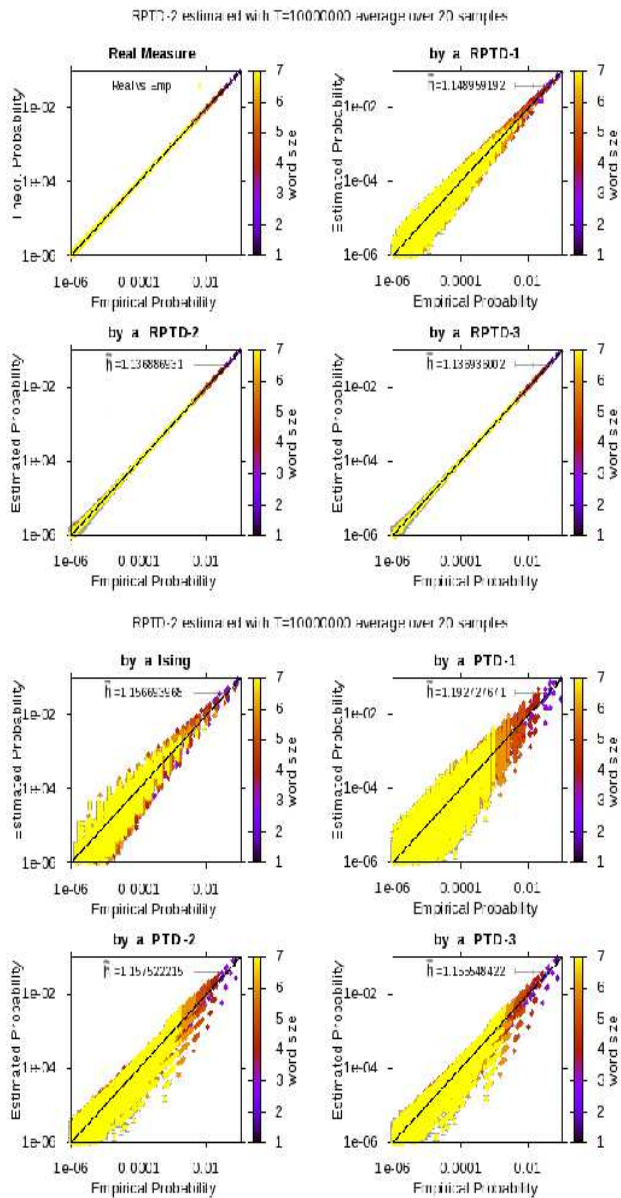


Figure 3: Figure 1 (top left) Expected probability μ_w versus empirical probability $\pi_w^{(T)}(w)$; Figure 2 (top right) to 8 (bottom right) Predicted probability versus empirical probability $\pi_w^{(T)}(w)$ for several models. The generating potential is a **RPTD-2**.

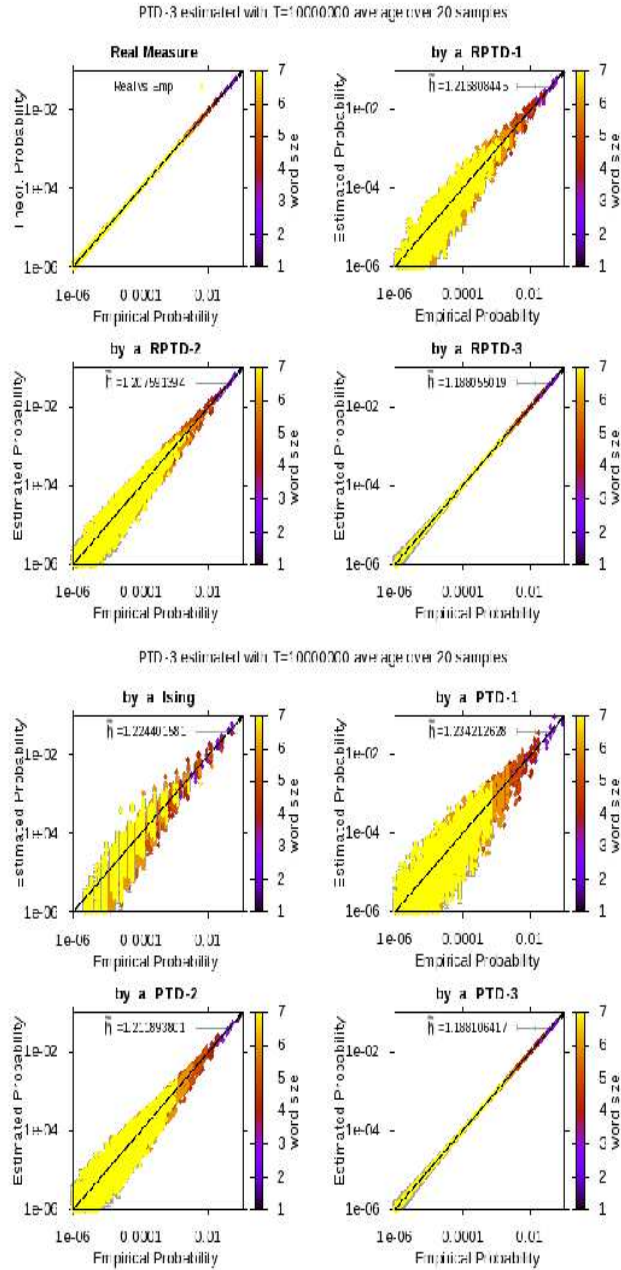


Figure 4: Same as previous figure where generating potential is a **PTD-3**.

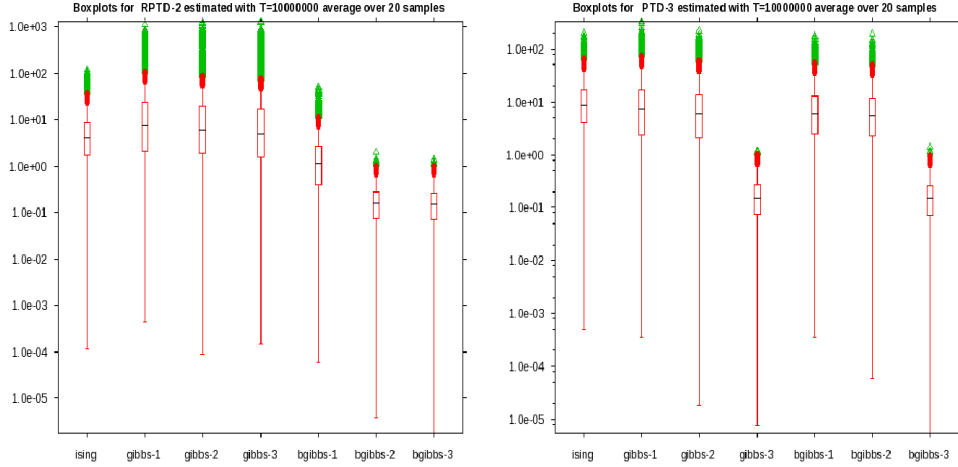


Figure 5: The box-plot (in log-scale) of the distributions of weighted deviations of word's probability versus their empirical probability, for several statistical models, using a generating potential of the form **(left) RPTD-2** and **(right) PTD-3**. Midliers Outliers (see footnote 25) are shown by red dots and extreme outliers by green dots.

χ^2 estimated value. Note that χ^2 test assumes Gaussian fluctuations about the mean value, which are satisfied for finite-range Gibbs distributions, as can be easily seen by expanding the large deviations function I_l in (32) up to the second order in ε . However, when comparing two different Gibbs distributions it might be that the deviations from the expected value of one Gibbs distribution compared to the expected value of the other Gibbs distribution is well beyond the mean-square deviation of the Gaussian fluctuations distribution, giving rise to huge χ^2 coefficients, as we see in the tables 3.

4.3 Spike train statistics in a simulated Neural Network

Here we simulate an Integrate-and-Fire neural network whose spike train statistics is explicitly and rigorously known [11] while effects of synaptic plasticity on statistics

Table 3: χ^2 coefficient calculated: (left) with all words of size < 7 ; (right) with words of size 7 only. See text for details.

Estimating \Generating	RPTD-2	PTD-3	Estimating \Generating	RPTD-2	PTD-3
Ising	135.427	415.965	Ising	121.825	347.502
PTD-1	3146.17	564.396	PTD-1	2839.36	468.763
PTD-2	3319.75	290.93	PTD-2	2537.39	229.255
PTD-3	2533.35	0.0571905	PTD-3	2053.72	0.057065
RPTD-1	13.9287	274.773	RPTD-1	11.6167	218.458
RPTD-2	0.0607027	223.516	RPTD-2	0.0605959	176.598
RPTD-3	0.0556114	0.0539691	RPTD-3	0.0553242	0.0541206

have been studied in [12].

4.3.1 Network dynamics.

The model is defined as follows. Denote by V_i the membrane potential of neuron i and W_{ij} the synaptic weight of neuron j over neuron i , I_i^{ext} an external input on neuron i . Each neuron is submitted to noise, modeled by an additional input, $\sigma_B B_i(t)$, with $\sigma_B > 0$ and where the $B_i(t)$'s are Gaussian, independent, centered random variable with variance 1. The network dynamics is given by:

$$V_i(t+1) = \gamma V_i(1 - Z[V_i(t)]) + \sum_{j=1}^N W_{ij} Z[V_j(t)] + I_i^{ext} + \sigma_B B_i(t); \quad i = 1 \dots N, \quad (39)$$

where $\gamma \in [0, 1[$ is the leak in this discrete time model ($\gamma = 1 - \frac{dt}{\tau}$). Finally, the function $Z(x)$ mimics a spike: $Z(x) = 1$ if $x \geq \theta = 1$ and 0 otherwise, where θ is the firing threshold. As a consequence, equation (39) implements both the integrate and firing regime. It turns out that this time-discretisation of the standard integrate-and-Fire neuron model, which as discussed in e.g. [33], provides a rough but realistic approximation of biological neurons behaviors. Its dynamics has been fully characterized for $\sigma_B = 0$ in [10] while the dynamics with noise is investigated in [11]. Its links to more elaborated models closer to biology is discussed in [13].

4.3.2 Exact spike trains statistics.

For $\sigma_B > 0$ there is a unique Gibbs distribution in this model, whose potential is explicitly known. It is given by:

$$\phi(\omega_{-\infty}^0) = \sum_{i=1}^N \left[\omega_i(0) \log \left(\pi \left(\frac{\theta - C_i(\underline{\omega})}{\sigma_i(\underline{\omega})} \right) \right) + (1 - \omega_i(0)) \log \left(1 - \pi \left(\frac{\theta - C_i(\underline{\omega})}{\sigma_i(\underline{\omega})} \right) \right) \right], \quad (40)$$

where $\pi(x) = \frac{1}{\sqrt{2\pi}} \int_x^{+\infty} e^{-\frac{u^2}{2}} du$, $\underline{\omega} = \omega_{-\infty}^{-1}$, $C_i(\underline{\omega}) = \sum_{j=1}^N W_{ij} x_{ij}(\underline{\omega}) + I_i^{ext} \frac{1 - \gamma^{t+1 - \tau_i(\underline{\omega})}}{1 - \gamma}$, $x_{ij}(\underline{\omega}) = \sum_{l=\tau_i(\underline{\omega})}^t \gamma^{t-l} \omega_j(l)$, $\sigma_i^2(\underline{\omega}) = \sigma_B^2 \frac{1 - \gamma^{2(t+1 - \tau_i(\underline{\omega}))}}{1 - \gamma^2}$. Finally, $\tau_i(\underline{\omega})$ is the last time, before $t = -1$, where neuron i has fired, in the sequence $\underline{\omega}$ (with the convention that $\tau_i(\underline{\omega}) = -\infty$ for the sequences such that $\omega_i(n) = 0, \forall n < 0$). This potential has infinite range but range $R \geq 1$ approximations exist, that consist of replacing $\underline{\omega} = \omega_{-\infty}^{-1}$ by ω_{-R}^{-1} in (40). The KL divergence between the Gibbs measure of the approximated potential and the exact measure decays like γ^R . Finite range potentials admit a polynomial expansion of form (5).

4.3.3 Numerical estimation of spike train statistics

Here we have considered only one example of model (39) (more extended simulations and results will be provided elsewhere). It consists of 4 neurons, with a *sparse* connectivity matrix so that there are neurons without synaptic interactions. The synaptic weights matrix is:

$$\mathcal{W} = \begin{pmatrix} 0 & -0.568 & 1.77 & 0 \\ 1.6 & 0 & -0.174 & 0 \\ 0 & 0.332 & 0 & -0.351 \\ 0 & 1.41 & -0.0602 & 0 \end{pmatrix},$$

while $\gamma = 0.1$, $\sigma_B = 0.25$, $I_i^{ext} = 0.5$.

First, one can compute directly the theoretical entropy of the model using the results exposed in the previous section: the entropy of the range- R approximation, that can be computed with our formalism, converges exponentially fast with R to the entropy of the infinite range potential. For these parameters, the asymptotic value is $h = 0.57$.

Then, we generate a raster of length $T = 10^7$ for the 4 neurons and we compute the KL divergence between the empirical measure and several potentials including:

- (i) The range- R approximation of (40), denoted $\phi^{(R)}$. Note that $\phi^{(R)}$ does not contain all monomials. In particular, *it does not have the Ising term (the corresponding coefficient is zero)*.
- (ii) A Bernoulli model ϕ^{Ber} ;
- (iii) An Ising model ϕ^{Is} ;
- (iv) A one-time step Ising Markov model (as proposed in [44]) ϕ^{MEDF} ²⁶;
- (v) A range- R model containing all monomials ϕ^{all} .

Here we can compute the KL divergence since we know the theoretical entropy. The results are presented in the table (4). Note that the estimated KL divergence of range-1 potentials slightly depend on R since the RPF operator, and thus the pressure, depend on R .

Table 4: Kullback-Leibler divergence between the empirical measure of a raster generated by (39) (See text for the parameters value) and the Gibbs distribution, for several statistical models.

	$\phi^{(R)}$	ϕ^{Ber}	ϕ^{Is}	ϕ^{MEDF}	ϕ^{all}
R=1	0.379	0.379	0.312	1.211	0.309
R=2	0.00883	0.299871	0.256671	0.257068	0.0075
R=3	-0.001	0.250736	0.215422	0.200534	0.0001

We observe that our procedure recovers the fact that the range- R potential $\phi^{(R)}$ is the best to approximate the empirical measure, in the sense that it minimizes the KL divergence and that it has the minimal number of terms (ϕ^{all} does as good as $\phi^{(R)}$ for the KL divergence but it contains more monomials whose coefficient (almost) vanish in the estimation).

²⁶or equivalently, a **RPTD**-1 from (37)

4.3.4 Synaptic plasticity.

Here the neural network with dynamics given by (39) has been submitted to the STDP rule (34). The goal is to check the validity of the statistical model given by (35), predicted in [12]. We use spike-trains of length $T = 10^7$ from a simulated network with $N = 10$ neurons.

Previous numerical explorations of the noiseless case, $\sigma_B = 0$, have shown [10, 13] that a network of N such neurons, with fully connected graph, where synapses are taken randomly from a distribution $\mathcal{N}(0, \frac{C^2}{N})$, where C is a control parameter, exhibits generically a dynamics with very large periods in determined regions of the parameters-space (γ, C) . On this basis, we choose; $N = 10$, $\gamma = 0.995$, $C = 0.2$. The external current $\mathbf{I}^{(ext)}$ in eq. (39) is given by $I_i^{ext} = 0.01$ while $\sigma_B = 0.01$. Note that fixing a sufficiently large average value for this current avoids a situation where neurons stops firing after a certain time (“neural death”).

We register the activity after 4000 steps of adaptation with the STPD rule proposed in (34). In this context we expect the potential for the whole population to be of the form (35) and for a subset of the population of the form (36). Therefore, we choose randomly 2 neurons among the N and we construct from them the prefix-tree. Then, for the 2 neuron potentials forms from (37), we estimate the coefficients that minimizes the Kullback-Leibler divergence. The probability of words of different sizes predicted by several statistical models from (37) versus empirical probability $\pi_\omega^{(T)}(w)$ obtained from a spike train and the corresponding \tilde{h} value of the estimation process for a fixed pair of neurons are shown on figure (4.3.4).

Results depicted on figure (4.3.4) show, on one hand, that the statistics is well fitted by (36). Moreover, the best statistical models, are those including rate terms (the differences between their KL value is two orders of magnitude smaller that within those not disposing of rate terms). We also note that for the words with the smallest probability values, the potential do not yields a perfect matching due to finite size effects (see fig (4.3.4)). Especially, the small number of events due to low firing rates of neurons makes more sensitive the relation between the length of observed sequences (word size) and the spike-train length necessary to provide a good sampling and hence a reliable empirical probability.

4.3.5 Additional tests: the non-stationary case

Here we present results of the parameter estimation method applied to a spike train with statistics governed by a non-stationary statistical model of range 1, i.e. with time varying coefficients for rate or synchronization terms. Since the generation of spike-trains corresponding to more general higher time-order non-stationary process is not trivial, these potentials with higher range values will be analyzed in a forthcoming paper.

In the following we use an Ising potential form (37) with time-varying coefficients $\psi = (\omega) = \lambda_1(t) \omega_1(0) + \lambda_2(t) \omega_2(0) + \lambda_3(t) \omega_1(0) \omega_2(0)$. The procedure to generate a non stationary spike-train of length T is the following. We fix a time dependent form for the 3 coefficients $\lambda_i(t)$. From the initial value of the λ_i 's (say at time t) we compute the invariant measure of the RPF operator. From this, we draw a Chapman-

Fit from BMS activity after 4000 STDP steps

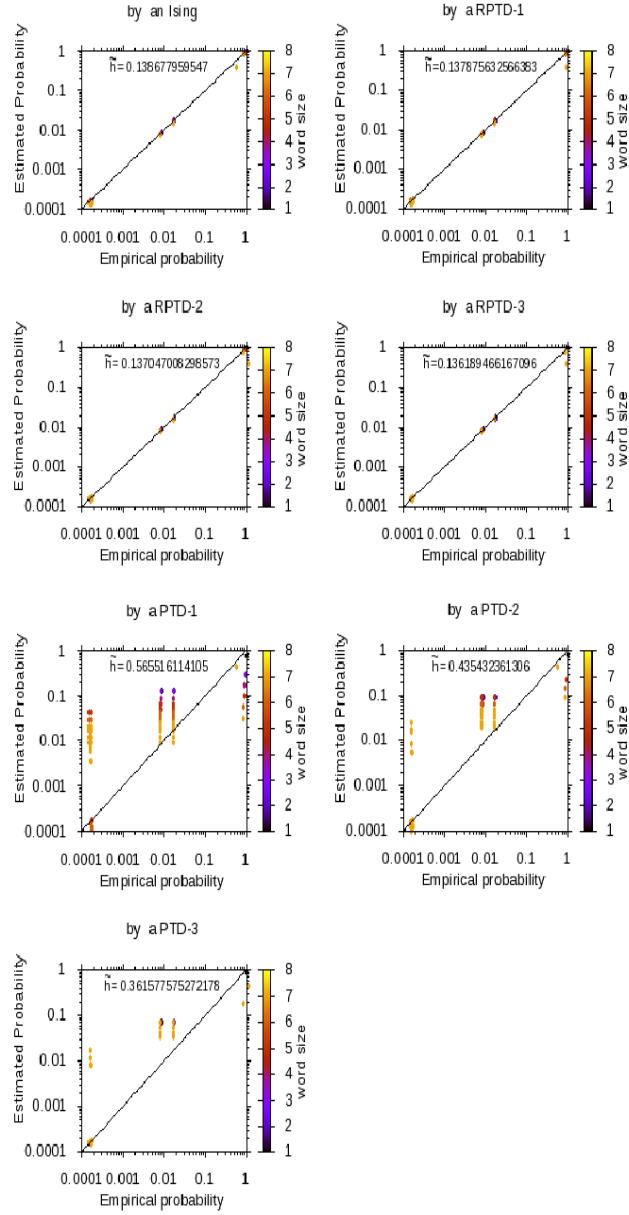


Figure 6: The probability of words of different sizes predicted by several statistical models from (37) versus empirical probability $\pi_{\omega}^{(T)}(w)$ obtained from a spike train generated by dynamics (39) after 4000 epochs of adaptation. The \hat{h} value (29) for each fitting model is shown inside the graphic. The potential is a pair potential of the form (36). Recall that **RPTD** Models include firing rates but **PTD** models do not.

Kolmogorov equation (20) with a time dependent RPF operator computed using the next coefficient values $\lambda_i(t+1)$.

With the generated spike-train, we perform the parameter estimation, but computing the empirical average over a small fraction of it which means a time window of size $T_0 = \frac{T}{M} \ll T$. Then, we slide the observation window and estimate again the coefficients value. We have verified that estimation procedure can recover correctly the coefficient values, for several types of time dependence, provided their variations be not too fast, and that the sliding window size be not too large with respect to T . We present the reconstruction of the parameters with a sinusoidal time-dependence given by $\lambda_0(t) = 0.4 + 0.3 \sin\left(\frac{4\pi t}{T-T_0}\right)$.

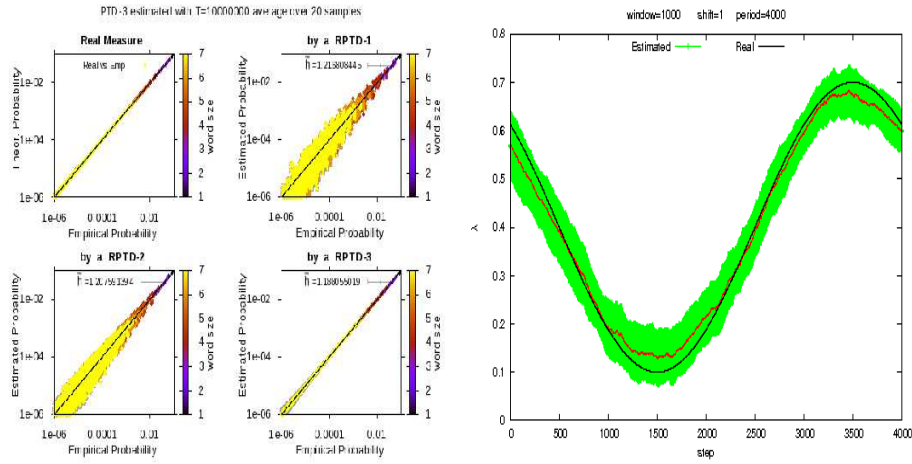


Figure 7: Estimation of coefficients on a Non-Stationary process genated by an Ising model and sinusoidal time dependence. Real value(black) and estimated parameter with its error bars (green) computed over 20 trials. The time shift is $\tau = 1$, Window size is fixed 1000, but oscillation period corresponds to 2000 (left) and 4000 (right).

5 Discussion and conclusion

5.1 Comparison with existing methods

Let us first summarize the advantages and drawbacks of our method compared with the existing ones. For this, we list some keywords in the approaches used by the community and discuss the links with our own work.

- **Maximum entropy.** The formalism that we use corresponds to a maximum entropy method but without limitations on the number or type of constraints. Actually, on mathematical grounds, it allows infinitely many constraints. Moreover, we do not need to compute the entropy.

- **Markovian approaches.** Our method is based on a Markovian approach where the memory depth of the Markov chain can be arbitrary long (actually the formalism that we use allows to theoretically consider processes with infinite memory, called *chains with complete connections* [43], see [11] for an application to spike train statistics). As we developed, the link between the potential extracted from the maximum entropy principle, by fixing *ad hoc* observables, and a Markov chain is not straightforward, since a potential of this kind is not normalized.
- **Monte-Carlo methods.** Equation (21) allows us to generate spike trains Gibbs-distributed with and arbitrary potential (non normalized). The convergence is ensured by eq. (14). We emphasize that we do not need to assume detailed balance. Instead, we impose a technical assumption (primitivity of the Ruelle-Perron-Frobenius matrix) which is more general than detailed balance. On the opposite, if this assumption does not hold then the unicity of the Gibbs distribution is not guaranteed and, in this case, the determination of spike train statistics from empirical data becomes even more cumbersome.
- **Determining an effective synaptic connectivity between neurons.** Interactions between neurons occur via synapses (or gap junction). This interaction is not instantaneous, it requires some delay. As a matter of fact, estimating the synaptic conductances via the spike statistics requires therefore to consider time-dependent potentials. Our formalism allows this. Determining an effective synaptic connectivity between neurons from spike trains will be the subject of a forthcoming paper.
- **Boltzmann learning.** Our approach can be viewed as “Boltzmann learning” (as presented e.g. in [61]) without restrictions on the parameters that we learn, without using a Monte Carlo approach (which assumes detailed balance), and uses a criterion which is strictly convex.
- **Performances.** At its current implementation level, the proposed method allows us to analyze the statistics of small groups (up to 8/12) of neurons. The parametric statistical potential of Markov processes up to range 16/20 is calculable, thus considering up to 2^{20} states for the process. The implementation considers several well-established numerical methods, in order to be applicable to a large set of possible data. With respect to the state of the art, this method allows us to consider non-trivial statistics (e.g. beyond rate models and even models with correlation), thus targeting models with complex spike patterns. This method is in a sense the next step after Ising models, known as being able to represent a large but limited part of the encoded information (e.g. [66, 48]). Another very important difference with respect to other current methods is that we perform the explicit variational optimization of a well defined quantity, i.e., the KL-divergence between the observed and estimated distributions. The method proposed here does not rely on Monte Carlo Markov Chain methods but on a spectral computation based on the RPF operator, providing exact formula, while the spectral characteristics are easily obtained from standard numerical methods.

The main drawback of our method is that it *does not allow to treat a large number of neurons and simultaneously a large range*. This is due to the evident fact that the number of monomials combinatorically increases as N, R growth. However, this is not a problem intrinsic to our approach but to parametric estimations potentials of the form (6). We believe that other form of potential could be more efficient (see [11] for an example). We also want to emphasize that, when considering Ising like statistics our algorithm is *less performant* than the existing ones (although improvements in speed and memory capacity thanks to the use of parallel computation algorithms remain an open and natural developpement path), for the simple reason that the latter has been developed and optimized using the tremendous results existing in statistical physics, for spins systems. Their extensions to models of the general form (6) seems rather delicate, as suggested by the nice work in [44] where extension between the 1-step Markov case is already cumbersome.

- **Mean-field methods.** Mean-field methods aim at computing the average value of observables (“order parameters”) relevant for the characterisation of statistical properties of the system. Typical examples are magnetisation in ferromagnetic models (corresponding to rates in spiking neurons models), but more elaborated order parameters are known e.g. in spin glasses [47] or in neural networks [75]. Those quantities obey equations (usually called mean-field equations) which are, in most cases, not explicetely solvable. Therefore, approximations are proposed from the simplest (naive mean-field equations) to more complex estimations, with significant results developed in the realm of spins systems (Ising model, Sherrington-Kirkpatrick spin glass model [71]). Examples are the replica method [47], Thouless-Anderson-Palmer equations [79], the Plefka expansion [77], or more recently e.g. the Sessak-Monasson approximation [70] (for a recent review on mean-field methods see [52]). Since the seminal paper by Schneidman and collaborators [67] they have also been applied to spike trains statistics analysis assuming that neurons dynamics generates a spike statistics characterized by a Gibbs distribution with an Ising Hamiltonian. In their most common form these methods do not consider dynamics (e.g time correlations) and their extension to the time-dependent case (e.g. dynamic mean-field methods) is far from being straightforward (see e.g. [76, 75, 3, 65, 24] for examples of such developments). Moreover, exact mean-field equations and their approximations usually only provide a probability measure at positive distance to the true (stationary) probability measure of the system (this distance can be quantified in the setting of information geometry using e.g. the KL distance [2]). This is the case whenever the knowledge of the sought order parameters is not sufficient to determine the underlying probability.

The present work can, in some sense, be interpreted in the realm of mean-field approaches. Indeed, we are seeking an hidden Gibbs measure and we have only information about the average value of ad hoc observables. Thus, equation (17) is a mean-field equation since it provides the average value of an observable with respect to the Gibbs distribution. There are therefore L such equations, where L is the number of monomials in the potential ψ . Are all these equations relevant

? If not, which one are sufficient to determine univoquely the Gibbs distribution ? Which are the order parameters ? The method consisting of providing a hierarchy of mean-field approximations which starts with the Bernoulli model (all monomials but the rate terms are replaced by a constant), then Ising (all monomials but rate and spatial correlations are replaced by a constant), while progressively diminishing the KL divergence allows to answer the question of the relevant order parameters and can be interpreted as well in the realm of information geometry. This hierarchical approach is a strategy to cope with the problem of combinatorial explosion of terms in the potential when the number of neurons or range increases. But the form of potential that we consider does not allow a straightforward application of the methods inherited from statistical mechanics of spin systems. As a consequence, we believe that instead of focusing too much on these methods it should be useful to adopt technics based on large deviations (which actually allows the rigorous fundation of dynamic mean field methods for spin-glasses [3] and neural networks [65, 24]). This is what the present formalism offers.

5.2 Conclusion and perspectives

The thermodynamic formalism allows us to provide closed-form calculations of interesting parameters related to spectral properties of the RPF operator. We, for instance, propose an indirect estimation of the entropy, via an explicit formula. We also provide numbers for the average values of the related observable, probability measure, etc.. This means that as soon as we obtain the numerical values of the Gibbs distribution up to some numerical precision, all other statistical parameters come for free without additional approximations.

A step further, the non-trivial but very precious virtue of the method is that it allows us to efficiently compare models. We thus not only estimate the optimal parameters of a model, but can also determine among a set of models which model is the most relevant. This means, for instance, that we can determine if either only rates, or rates and correlations matters, for a given piece of data. Another example is to detect if a given spike pattern is significant, with respect to a model not taking this pattern into account. The statistical significance mechanism provides numbers that are clearly different for models corresponding or not to a given empirical distribution, providing also an absolute test about the estimation significance. These elements push the state of the art regarding statistical analysis of spike train a step further.

At the present state of the art, the present method is limited by three bounds.

First of all, the formalism is developed for a stationary spike-train, i.e. for which the statistical parameters are constant. This is indeed a strong limitation, especially in order to analyze biological data, though several related approaches consider the same restrictive framework. This drawback is overcome at two levels. At the implementation level we show here how using a sliding estimation window and assuming an adiabatic, i.e. slowly varying, distribution we still can perform some relevant estimation. In a nutshell, the method seems still usable and we are now currently investigating this on both simulated and biological data, this being another study on its own. At a more

theoretical level, we are revisiting the thermodynamic formalism developed here for time varying parameters (in a similar way as the so called inhomogeneous Poisson process with time varying rates). Though this yields non-trivial developments beyond the scope of this work, it seems that we can generalize the present formalism in this direction.

Secondly, the present implementation has been optimized for dense statistical distributions, i.e., in the case where almost all possible spike combinations are observed. Several mechanisms, such as look-up tables, make this implementation very fast. However, if the data is sparse, as it may be the case for biological, a dual implementation has to be provided using data structure, such as associative tables, well adapted to the fact that only a small amount of possible spike combinations are observed. This complementary implementation has been made available and validated against the present one. This is going to analyze sparse Markov processes up to range much higher than $16/20$. Again this is not a trivial subject and this aspect must be developed in a next study as well as the applicability of parallel computing alternatives (e.g. sparse matrix storage, parallel fast-eigenvalue algorithms, etc.).

Finally, given an assembly of neurons, every statistical tools available today provide only the analysis of the statistics a small subset of neurons, and it is known that this only partially reflects the behavior of the whole population [40]. The present method for instance, is difficult to generalize to more than $8/10$ neurons because of the incompressible algorithmic complexity of the formalism although parallel computation techniques might be helpful. However, the barrier is not at the implementation level, but at the theoretical level, since effective statistical general models (beyond Ising models) allow for instance to analyze statistically large spiking patterns such as those observed in synfire chains [30] or polychronism mechanisms [54]. This may be the limit of the present class of approaches, and things are to be thought differently. We believe that the framework of thermodynamic formalism and links to Statistical Physics is still a relevant source of methods for such challenging perspectives.

acknowledgements

We are grateful to F. Grammont, C. Malot, F. Delarue and P. Reynaud-Bourret for helpful discussions and Adrien Palacios for his precious remarks and profound scientific questions at the origin of main aspects of the present work. Partially supported by the ANR MAPS & the MACACC ARC projects and PhD.D-fellowship from Research Ministry to J.C Vasquez.

References

- [1] Moshe Abeles and George L. Gerstein. Detecting spatiotemporal firing patterns among simultaneously recorded single neurons. *Journal of Neurophysiology*, 60(3):909–924, September 1988.
- [2] Shun-Ichi Amari and H. Nagaoka. *Methods of Information Geometry*. Oxford Univ. Press., 2000.
- [3] G. BenArous and A. Guionnet. Large deviations for langevin spin glass dynamics. *Probability Theory and Related Fields*, 102:455–509, 1995.
- [4] G. Bi and M. Poo. Synaptic modification by correlated activity: Hebb’s postulate revisited. *Annual Review of Neuroscience*, 24:139–166, March 2001.

- [5] R. Bowen. *Equilibrium states and the ergodic theory of Anosov diffeomorphisms. Second revised version.*, volume 470 of *Lect. Notes in Math.* Springer-Verlag, 2008.
- [6] P. C. Bressloff and S. Coombes. *Synchronization of synaptically-coupled neural oscillators in: Epilepsy as a dynamic disease*, chapter 7. J. Milton and P. Jung, Springer-Verlag, 2003.
- [7] D. R. Brillinger. Maximum likelihood analysis of spike trains of interacting nerve cells. *Biol Cybern*, 59(3):189–200, 1988.
- [8] Emery N. Brown, Robert E. Kass, and Partha P. Mitra. Multiple neural spike train data analysis: state-of-the-art and future challenges. *Nature Neuroscience*, 7(5):456–461, May 2004.
- [9] B. Cessac. Does the complex susceptibility of the h enon map have a pole in the upper-half plane ? a numerical investigation. *Nonlinearity*, 20:2883–2895, dec 2007.
- [10] B. Cessac. A discrete time neural network model with spiking neurons. i. rigorous results on the spontaneous dynamics. *J. Math. Biol.*, 56(3):311–345, 2008.
- [11] B. Cessac. A discrete time neural network model with spiking neurons ii. dynamics with noise. *J. Math. Biol.*, *accepted*, 2010.
- [12] B. Cessac, H. Rostro-Gonzalez, J.C. Vasquez, and T. Vi eville. How gibbs distribution may naturally arise from synaptic adaptation mechanisms: a model based argumentation. *J. Stat. Phys.*, 136(3):565–602, August 2009.
- [13] B. Cessac and T. Vi eville. On dynamics of integrate-and-fire neural networks with adaptive conductances. *Frontiers in neuroscience*, 2(2), jul 2008.
- [14] J.R. Chazottes. *Entropie Relative, Dynamique Symbolique et Turbulence*. PhD thesis, Universit  de Provence - Aix Marseille I, 1999.
- [15] J.R. Chazottes, E. Floriani, and R. Lima. Relative entropy and identification of gibbs measures in dynamical systems. *J. Statist. Phys.*, 90(3-4):697–725, 1998.
- [16] J.R. Chazottes and G. Keller. *Pressure and Equilibrium States in Ergodic Theory*, chapter Ergodic Theory. Encyclopedia of Complexity and System Science, Springer, 2009. to appear.
- [17] Sung Nok Chiu and Kwong Ip Liu. Generalized cram r-von mises goodness-of-fit tests for multivariate distributions. *Computational Statistics and Data Analysis*, 53(11):3817–3834, 2009.
- [18] E. S. Chornoboy, L. P. Schramm, and A. F. Karr. Maximum likelihood identification of neural point process systems. *Biol Cybern*, 59(4-5):265–275, 1988.
- [19] Simona Cocco, Stanislas Leibler, and R mi Monasson. Neuronal couplings between retinal ganglion cells inferred by efficient inverse statistical physics methods. *Proceedings of the National Academy of Sciences of the United States*, 106(33):14058–14062, August 2009.
- [20] Noel Cressie and Timothy R. C. Read. Multinomial goodness-of-fit tests. *Journal of the Royal Statistical Society. Series B (Methodological)*, 46(3):440–464, 1984.
- [21] Imre Csiszar. Sanov property, generalized i -projection and a conditional limit theorem. *Ann. Prob.*, 12(3):768–793, 1984.
- [22] Amir Dembo and Ofer Zeitouni. *Large Deviation Techniques and Applications*. Springer, 1993.
- [23] M. Diesmann, M-O. Gewaltig, and A. Aertsen. Stable propagation of synchronous spiking in cortical neural networks. *Nature*, 402:529–533, 1999.
- [24] O. Faugeras, J. Touboul, and B. Cessac. A constructive mean field analysis of multi population neural networks with random synaptic weights and stochastic inputs. *Frontiers in Neuroscience*, 2008. submitted.
- [25] Michael Frigge, David C Hoaglin, and Boris Iglewicz. Implementation of the boxplot. *The American Statistician*, 43(1):50–54, February 1989.
- [26] Yun Gao, Ioannis Kontoyiannis, and Elie Bienenstock. Estimating the entropy of binary time series: Methodology, some theory and a simulation study. *Entropy*, 10(2):71–99, 2008.
- [27] I.I. Gikhman and A.V. Skorokhod. *The Theory of Stochastic Processes*. Springer, 1979.

- [28] F. Grammont and A. Riehle. Precise spike synchronization in monkey motor cortex involved in preparation for movement. *Exp. Brain Res.*, 128:118–122, 1999.
- [29] Peter Grassberger. Estimating the information content of symbol sequences and efficient codes. *IEEE Transactions on Information Theory*, 35, 1989.
- [30] J. Hertz. *Theoretical Aspects of Neural Computation.*, chapter Modelling synfire processing., pages 135–144. Wong K-Y M. King I. and Yeung D-Y (eds), Springer-Verlag, 1997.
- [31] A.L. Hodgkin and A.F. Huxley. A quantitative description of membrane current and its application to conduction and excitation in nerve. *Journal of Physiology*, 117:500–544, 1952.
- [32] Aapo Hyvärinen. Estimation of non-normalized statistical models by score matching. *J. Mach. Learn. Res.*, 6:695–709, 2005.
- [33] E. Izhikevich. Simple model of spiking neurons. *IEEE Transactions on Neural Networks*, 14(6):1569–1572, 2003.
- [34] E.T. Jaynes. Information theory and statistical mechanics. *Phys. Rev.*, 106:620, 1957.
- [35] Don H. Johnson and Ananthram Swami. The transmission of signals by auditory-nerve fiber discharge patterns. *J. Acoust. Soc. Am*, 74(2):493–501, August 1983.
- [36] R. E. Kass and V. Ventura. A spike-train probability model. *Neural Comput.*, 13(8):1713–1720, 2001.
- [37] Robert E. Kass, Valrie Ventura, and Emery N. Brown. Statistical issues in the analysis of neuronal data. *Journal of Neurophysiology*, 94(1):8–25, January 2005.
- [38] G. Keller. *Equilibrium States in Ergodic Theory*. Cambridge University Press, 1998.
- [39] Kathryn Laskey and Laura Martignon. Bayesian learning of loglinear models for neural connectivity. In *Proceedings of the Twelfth Conference Annual Conference on Uncertainty in Artificial Intelligence (UAI-96)*, pages 373–380, San Francisco, CA, 1996. Morgan Kaufmann.
- [40] P.E. Latham, A. Roth, M. Hausser, and M. London. Requiem for the spike? *Soc. Neurosc. Abstr.*, 32, 2006.
- [41] BG Lindsey, KF Morris, R Shannon, and GL Gerstein. Repeated patterns of distributed synchrony in neuronal assemblies. *Journal of Neurophysiology*, 78:1714–1719, 1997.
- [42] Michael London, Adi Shreibman, and Idan Segev. Estimating information theoretic quantities of spike-trains using the context tree weighting algorithm. *Nature neuroscience*, 5, 2002. Appendix to: The information efficacy of a synapse.
- [43] G. Maillard. *Introduction to chains with complete connections*. Ecole Federale Polytechnique de Lausanne, winter 2007.
- [44] Olivier Marre, Sami El Boustani, Yves Frégnac, and Alain Destexhe. Prediction of spatiotemporal patterns of neural activity from pairwise correlations. *Physical Review Letters*, 102(13):4, April 2009.
- [45] Laura Martignon, Gustavo Deco, Kathryn Laskey, Mathiew Diamond, Winrich Freiwald, and Eilon Vaadia. Neural coding: Higher-order temporal patterns in the neurostatistics of cell assemblies. *Neural Computation*, 12(11):2621–2653, November 2000.
- [46] Laura Martignon, H. von Hasseln, S. Grün, A. Aertsen, and G. Palm. Detecting higher-order interactions among the spiking events in a group of neurons. *Biological Cybernetics*, 73(1):69–81, July 1995.
- [47] M. Mézard, G. Parisi, and M.A. Virasoro. *Spin-glass theory and beyond*. World scientific Singapore, 1987.
- [48] Marc Mezard and Thierry Mora. Constraint satisfaction problems and neural networks: A statistical physics perspective. *Journal of Physiology-Paris*, 103(1–2):107–113, January–March 2009.
- [49] Gusztáv Morvai and Benjamin Weiss. Estimating the lengths of memory words. *IEEE TRANSACTIONS ON INFORMATION THEORY*, 54(8):3804–3807, august 2008.
- [50] A.V. Negaev. An asymptotic formula for the neyman-pearson risk in discriminating between two markov chains. *Journal of Mathematical Sciences*, 111(3):3582–3591, 2002.
- [51] Murat Okatan, Matthew A. Wilson, and Emery N. Brown. Analyzing functional connectivity using a network likelihood model of ensemble neural spiking activity. *Neural Computation*, 17(9):1927–1961, September 2005.

- [52] Manfred Opper and David Saad. *Advanced Mean Field Methods: Theory and Practice*. MIT. Press., 2001.
- [53] Leslie C. Osborne, Stephanie E. Palmer, Stephen G. Lisberger, and William Bialek. The neural basis for combinatorial coding in a cortical population response. *The Journal of Neuroscience*, 28(50):13522–13531, December 2008.
- [54] Hélène Paugam-Moisy, Régis Martinez, and Samy Bengio. Delay learning and polychronization for reservoir computing. *Neurocomputing*, 71:1143–1158, 2008.
- [55] Alexandre Pouget and Gregory C DeAngelis. Paying attention to correlated neural activity. *Nature Neuroscience*, 11(12):1371–1372, December 2008.
- [56] C. Pouzat and A. Chaffiol. On goodness of fit tests for models of neuronal spike trains considered as counting processes. <http://arxiv.org/abs/0909.2785v1>, 2009.
- [57] Christophe Pouzat and Antoine Chaffiol. Automatic spike train analysis and report generation. an implementation with r, r2html and star. *J Neurosci Methods*, 181:119–144, 2009.
- [58] Christophe Pouzat and Antoine Chaffiol. On goodness of fit tests for models of neuronal spike trains considered as counting processes, 2009.
- [59] F. Rieke, D. Warland, R. de Ruyter van Steveninck, and W. Bialek. *Spikes: Exploring the Neural Code*. Bradford Books, 1997.
- [60] Yasser Roudi, Erik Aurell, and John A Hertz. Statistical physics of pairwise probability models. *Frontiers in Computational Neuroscience*, page 15, 2009.
- [61] Yasser Roudi, Joanna Tyrcha, and John A Hertz. Ising model for neural data: model quality and approximate methods for extracting functional connectivity. *Physical Review E*, page 051915, 2009.
- [62] D. Ruelle. Statistical mechanics of a one-dimensional lattice gas. *Commun. Math. Phys.*, 9:267–278, 1968.
- [63] D. Ruelle. *Statistical Mechanics: Rigorous results*. Benjamin, New York, 1969.
- [64] D. Ruelle. *Thermodynamic formalism*. Addison-Wesley, Reading, Massachusetts, 1978.
- [65] M. Samuelides and B. Cessac. Random recurrent neural networks. *European Physical Journal - Special Topics*, 142:7–88, 2007.
- [66] E. Schneidman, M.J. Berry, R. Segev, and W. Bialek. Weak pairwise correlations imply string correlated network states in a neural population. *Nature*, 440:1007–1012, 2006.
- [67] E. Schneidman, M.J. Berry, R. Segev, and W. Bialek. Weak pairwise correlations imply strongly correlated network states in a neural population. *Nature*, 440(7087):1007–1012, 2006.
- [68] Thomas Schürmann and Peter Grassberger. Entropy estimation of symbol sequences. *Chaos*, 6(3):414–427, 1996.
- [69] R. Segev, I. Baruchi, E. Hulata, and E. Ben-Jacob. Hidden neuronal correlations in cultured networks. *Physical Review Letters*, 92:118102, 2004.
- [70] sessak V. and Remi Monasson. Small-correlation expansions for the inverse ising problem. *J. Phys. A*, 42:055001, 2009.
- [71] D. Sherrington and S. Kirkpatrick. Solvable model of a spin-glass. *Physical Review Letters*, 35(26):1792+, December 1975.
- [72] Jonathon Shlens, Greg D. Field, Jeffrey L. Gauthier, Martin Greschner, Alexander Sher, Alan M. Litke, and E. J. Chichilnisky. The structure of large-scale synchronized firing in primate retina. *The Journal of Neuroscience*, 29(15):5022–5031, April 2009.
- [73] Jonathon Shlens, Greg D. Field, Jeffrey L. Gauthier, Matthew I. Grivich, Dumitru Petrusca, Alexander Sher, Alan M. Litke, and E. J. Chichilnisky. The structure of multi-neuron firing patterns in primate retina. *The Journal of Neuroscience*, 26(32):8254–8266, August 2006.
- [74] Ya Sinai. Gibbs measures in ergodic theory. *Russ. Math. Surveys*, 27(4):21–69, 1972.
- [75] H. Sompolinsky, A. Crisanti, and H.J. Sommers. Chaos in random neural networks. *Phys. Rev. Lett.*, 61:259–262, 1988.

- [76] H. Sompolinsky and A. Zippelius. Relaxational dynamics of the Edwards-Anderson model and the mean-field theory of spin-glasses. *Physical Review B*, 25(11):6860–6875, 1982.
- [77] Plefka T. Convergence condition of the tap equations for the infinite-ranged ising spin glass model. *J. Phys. A*, 15:1971, 1982.
- [78] Anon Tang1, David Jackson, Jon Hobbs, Wei Chen, Jodi L. Smith, Hema Patel, Anita Prieto, Dumitru Petrusca, Matthew I. Grivich, Alexander Sher, Pawel Hottowy, Wladyslaw Dabrowski, Alan M. Litke, and John M. Beggs. A maximum entropy model applied to spatial and temporal correlations from cortical networks *In Vitro. The Journal of Neuroscience*, 28(2):505–518, January 2008.
- [79] D. J. Thouless, P. W. Anderson, and R. G. Palmer. Solution of a solvable model of a spin glass. *Philos. Mag.*, 35:593–601, 1977.
- [80] Gašper Tkačik, Elad Schneidman, Michael J. Berry II, and William Bialek. Ising models for networks of real neurons. *arXiv*, page 4, 2006.
- [81] Wilson Truccolo and John P. Donoghue. Nonparametric modeling of neural point processes via stochastic gradient boosting regression. *Neural Computation*, 19(3):672–705, 2007.
- [82] Wilson Truccolo, Uri T. Eden, Matthew R. Fellows, John P. Donoghue, and Emery N. Brown. A point process framework for relating neural spiking activity to spiking history, neural ensemble and extrinsic covariate effects. *J Neurophysiol*, 93:1074–1089, 2005.
- [83] Alessandro E. P. Villa, , Igor V. Tetko, Brian Hyland, and Abdellatif Najem. Spatiotemporal activity patterns of rat cortical neurons predict responses in a conditioned task. *Proc Natl Acad Sci USA*, 96(3):1106–1111, 1999.

